

CHAPTER 4

Development of a Tandem Conjugate Addition/Prins Cyclization

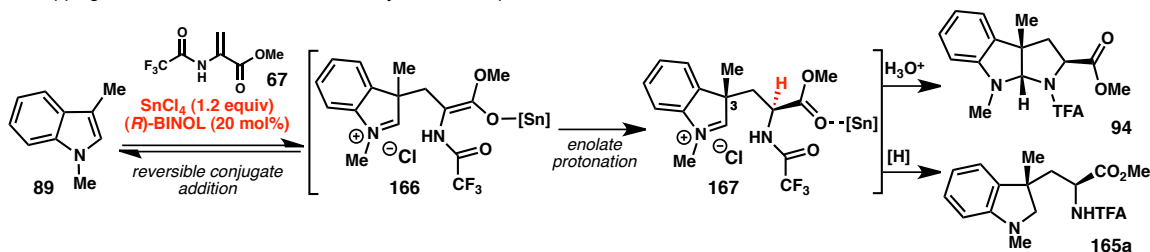
4.1 Introduction

Mechanistic studies of the formal (3 + 2) cycloaddition between 3-substituted indoles and 2-amidoacrylates revealed that the initial product is an iminium ion, and cyclization by the pendant amide to afford the pyrroloindoline occurs upon aqueous work-up (Chapter 2). As a result, we hypothesized that novel indoline structures could be accessed by intercepting the iminium ion with alternate nucleophiles. Chapter 3 described the use of reducing agents for this purpose; this chapter will discuss our investigation of carbon nucleophiles (Figure 1a).

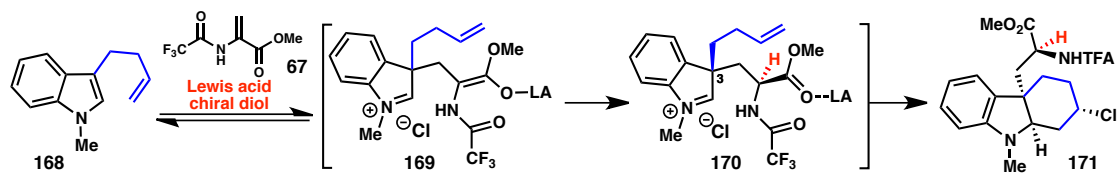
Our initial goal was the development of an intramolecular cascade reaction. We envisioned that upon Lewis acid promoted conjugate addition of the indole to the acrylate, a tethered alkene would add into the iminium intermediate. The resulting carbocation would then be quenched by a nucleophile such as chloride. Overall, such a reaction would constitute a tandem conjugate addition/asymmetric protonation/Prins cyclization (Figure 1b).

Figure 1. a) Previously developed pyrroloindoline and indoline syntheses. b) Proposed conjugate addition/Prins cyclization.

a. Trapping of indolinium ion with amide and hydride nucleophiles



b. Conjugate addition/Prins cyclization

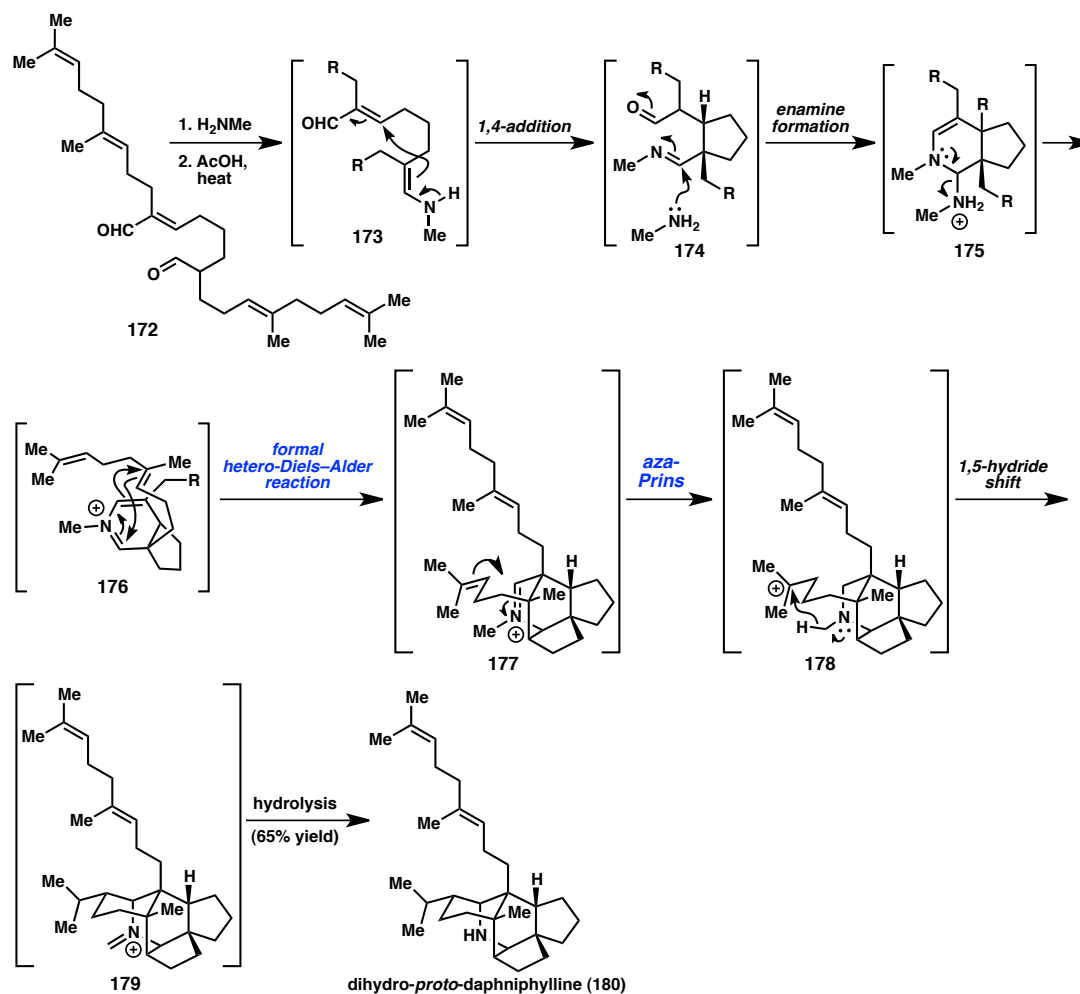


4.1.1 Cascade Reactions Incorporating Prins Cyclizations

Cascade reactions have long attracted the attention of organic chemists with their ability to rapidly build up molecular complexity. Several groups have reported examples of cascades either initiated by or terminated with a Prins cyclization. Heathcock and coworkers' one-step synthesis of dihydro-*proto*-daphniphylline involves an incredible cascade of iminium ion intermediates, including a formal hetero-Diels–Alder reaction (which likely proceeds in a stepwise manner), followed by an aza-Prins cyclization to generate carbocation **178** (Figure 2).¹

Figure 2. Iminium cascade with a Prins cyclization by Heathcock.

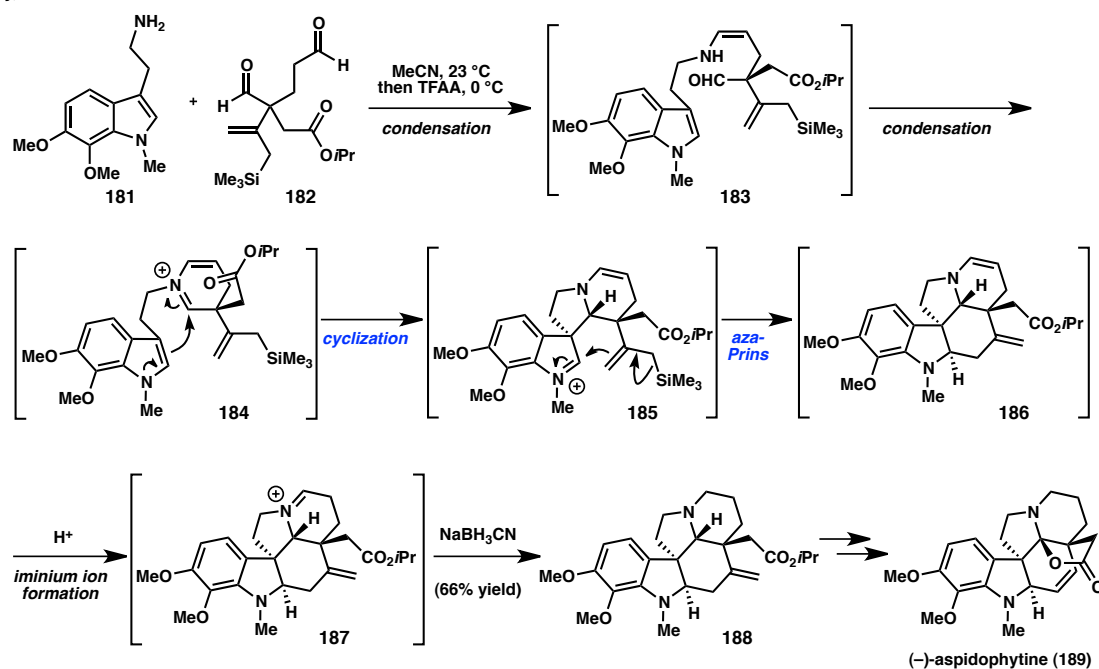
Heathcock, 1992



Another cascade of iminium ions was utilized by Corey and coworkers to enable an efficient synthesis of aspidophytine (Figure 3).² Cyclization of iminium ion **184** forms the C3 quaternary stereocenter and generates indolinium ion **185**. The stereoselectivity observed in this reaction may result from an interaction between the iminium ion carbon and the ester carbonyl oxygen of **184**, leading to preferential attack by the indole from the opposite face. The stereochemistry of spirocyclic intermediate **185** determines the facial selectivity of allylsilane attack in the subsequent aza-Prins cyclization.

Figure 3. Cascade with Prins cyclization in synthesis of (–)-aspidoptytine.

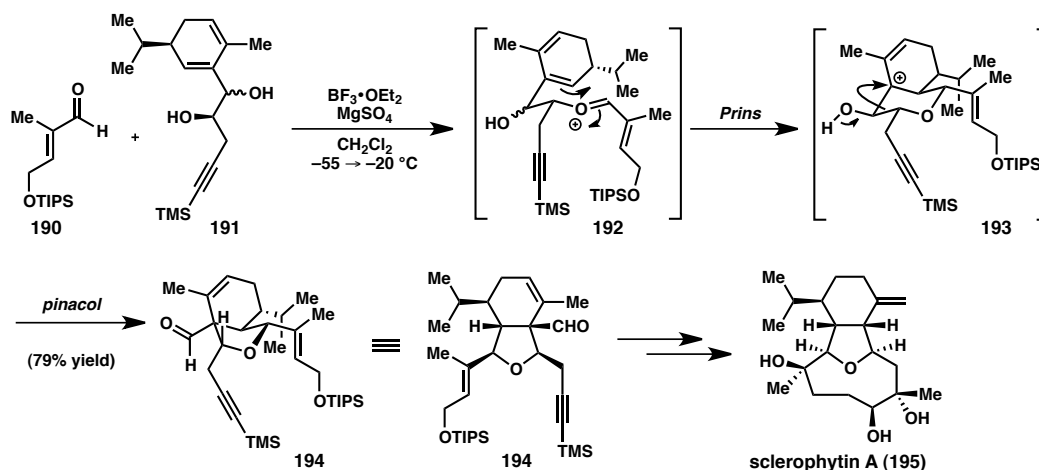
Corey, 1999



The pinacol-terminated Prins cyclization was developed by the Overman group and has facilitated the total syntheses of several natural products. One such application is found in their synthesis of sclerophytin A, part of the cladiellin family of diterpene metabolites (Figure 4).³ Lewis acid catalyzed condensation of diol **191** with aldehyde **190** forms oxocarbenium **192**. While either hydroxyl group can participate in this step, the condensation is reversible and only product **192** can carry on in the subsequent Prins cyclization. The bulky isopropyl substituent controls the stereoselectivity of this Prins cyclization, which generates allylic carbocation **193**. The cascade is terminated by a pinacol rearrangement to afford bicycle **194**.

Figure 4. Prins-pinacol in synthesis of sclerophytin A.

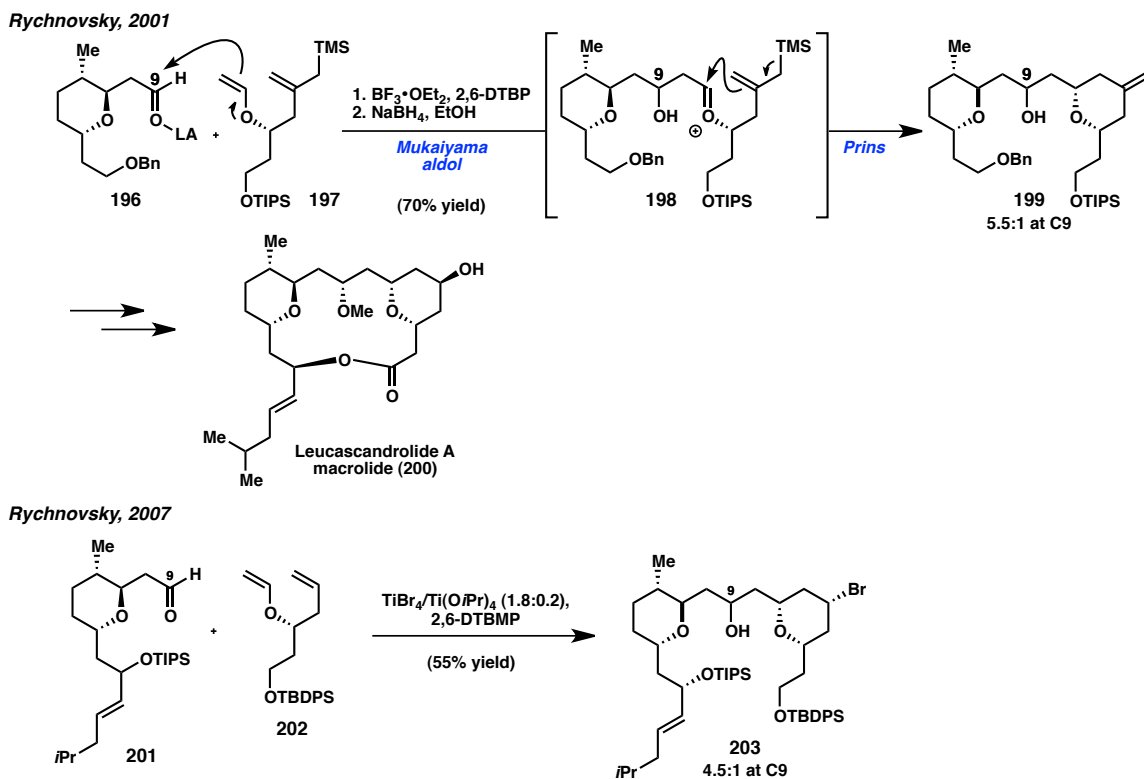
Overman, 2001



Rychnovsky and coworkers developed a Mukaiyama aldol-Prins cyclization cascade, and demonstrated the utility of this transformation in a formal synthesis of leucascandrolide A (Figure 5).⁴ Chiral aldehyde **196** and enol ether **197** underwent aldol-Prins coupling in the presence of 2.5 equivalents of $\text{BF}_3 \cdot \text{OEt}_2$ and 1.5 equivalents of 2,6-di-*tert*-butylpyridine to produce most of the leucascandrolide A skeleton in a single step.

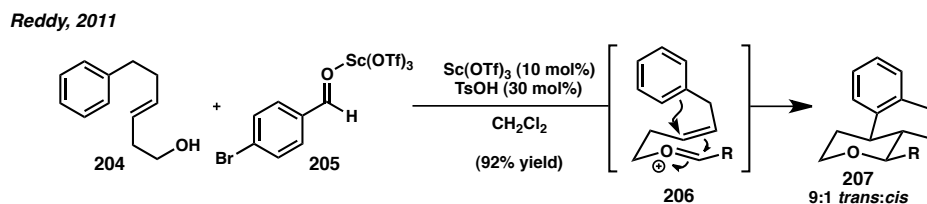
In 2007, the Rychnovsky laboratory reported a streamlined synthesis of leucascandrolide A using an improved variant of the Mukaiyama aldol-Prins coupling.⁵ The second generation methodology utilizes more accessible cyclization precursors (**201** and **202**) rather than an enol ether allylsilane, and yields a more highly functionalized product (**203**) with three new stereocenters (Figure 5).

Figure 5. Mukaiyama aldol-Prins in formal synthesis of leucascandrolide A.



Reddy and coworkers developed a Prins/Friedel–Crafts cyclization to access fused tricyclic systems (Figure 6).⁶ The stereochemistry of the product is determined by the olefin geometry in the starting material. However, a small amount of the minor, *cis* diastereomer is formed through a stepwise mechanism in the case shown in Figure 6.

Figure 6. Prins-Friedel–Crafts by Reddy.

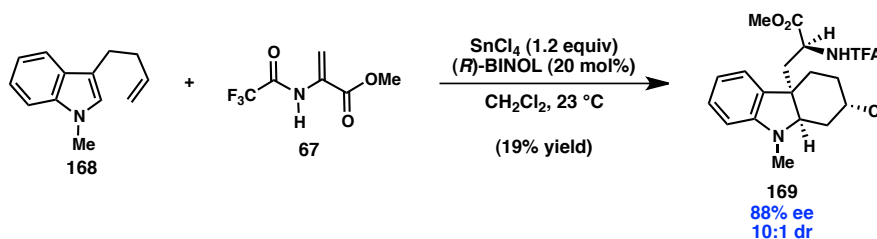


4.2 Development of a Conjugate Addition/Prins Cyclization

Although many examples exist in the literature of cascade reactions involving Prins cyclizations, a Prins cyclization triggered by a conjugate addition/asymmetric enolate protonation was not known at the outset of this project.

Preliminary studies showed that exposure of 3-homoallyl indole **168** and acrylate **67** to SnCl₄ and (*R*)-BINOL yields indoline **169** with a highly promising 88% ee, but low yield due to the formation of side products (Figure 7). A chloride ion from the Lewis acid serves to quench the carbocationic intermediate. While the reaction conditions are similar to the formal (3 + 2) cycloaddition, pyrroloindoline formation is precluded by addition of the tethered alkene to the indolinium ion during the course of the reaction.

Figure 7. Preliminary result for conjugate addition/Prins cyclization.



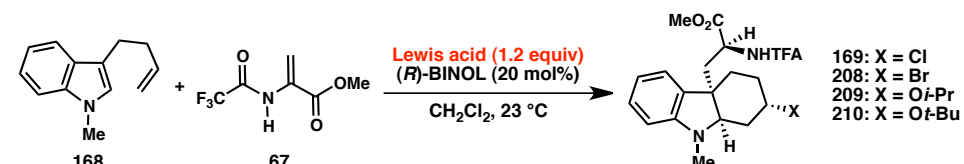
4.2.1 Catalyst Optimization

In order to improve the yield of this reaction, a screen of Lewis acids was conducted (Table 1). While tin tetrachloride provided us with our initial hit (entry 1), tin tetrabromide failed to give any of the desired Prins product (entry 2). Titanium tetrachloride provided the desired product in 27% yield and 6:1 dr, but as a racemic mixture (entry 3). Titanium isopropoxide, which would afford the product of isopropoxide-trapping of the intermediate carbocation, failed to promote this reaction

(entry 4). On the other hand, zirconium tetrachloride provided the product in 30% yield, 9:1 dr, and 40% ee (entry 5). Zirconium tert-butoxide was not an effective Lewis acid for this reaction (entry 6), while antimony pentachloride proved to be too reactive, and only indole decomposition was observed, even at $-78\text{ }^{\circ}\text{C}$ (entry 7).

While the enantioselectivity observed with zirconium tetrachloride was lower than with tin tetrachloride, the reaction was qualitatively much cleaner, with fewer side products. Thus, subsequent optimization was performed with zirconium tetrachloride.

Table 1. Lewis acid screen.

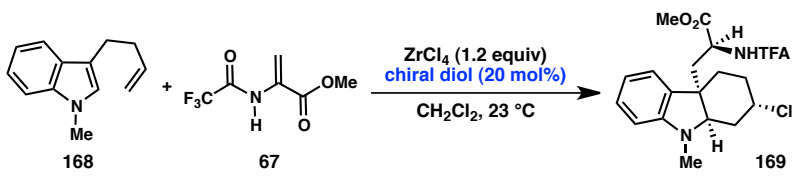


Entry	Lewis acid	Product	Yield (%)	ee (%) ^a
1	SnCl ₄	169	19	88
2	SnBr ₄	208	0	--
3	TiCl ₄	169	27	0
4	Ti(O ⁱ Pr) ₄	209	0	--
5	ZrCl ₄	169	30	40
6	Zr(O ^t Bu) ₄	210	0	--
7	SbCl ₅	169	0	--

Next, a ligand screen was performed (Table 2). While electronic perturbation of the BINOL backbone with bromine substituents at the 6 and 6' positions failed to improve yield and ee, bromine substituents at the 3 and 3' positions, which would have both an electronic and steric influence, resulted in greatly improved ee. (*S*)-VANOL gave a similarly high levels of enantioinduction, but its high cost and difficulty in preparation make it less desirable than 3,3'-Br₂-BINOL. (*S*)-VAPOL did not yield any product, presumably due to steric hindrance, while no enantioselectivity was observed with

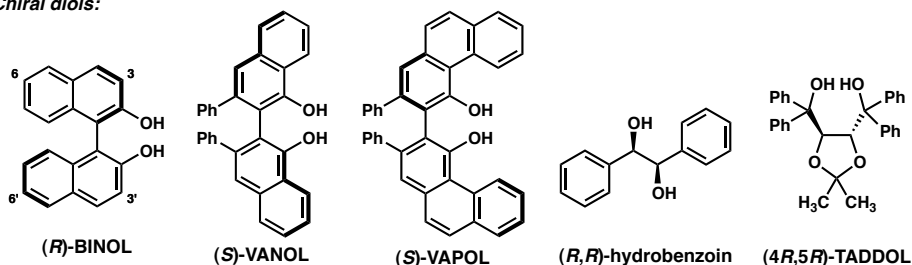
hydrobenzoin. TADDOL appeared initially promising, providing indoline **169** in 37% yield and 66% ee, but subsequent screening revealed decomposition under the reaction conditions. Thus (*R*)-3,3'-Br₂-BINOL was determined to be the optimal ligand for this transformation.

Table 2. Ligand screen.



Entry	Chiral Diol	Yield (%)	ee (%) ^a
1	(<i>R</i>)-BINOL	30	40
2	(<i>R</i>)-6,6'-Br ₂ -BINOL	38	30
3	(<i>R</i>)-3,3'-Br ₂ -BINOL	40	76
4	(<i>S</i>)-VANOL	33	74
5	(<i>S</i>)-VAPOL	0	--
6	(<i>R,R</i>)-hydrobenzoin	35	0
7	(4 <i>R,5R</i>)-TADDOL	37	66

Chiral diols:

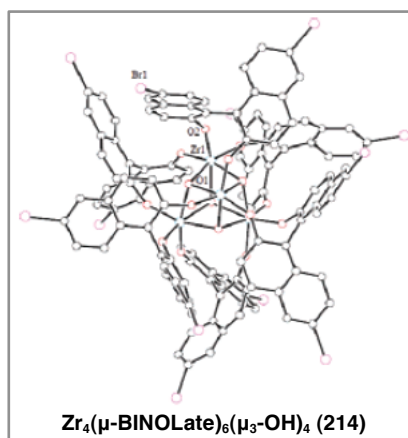
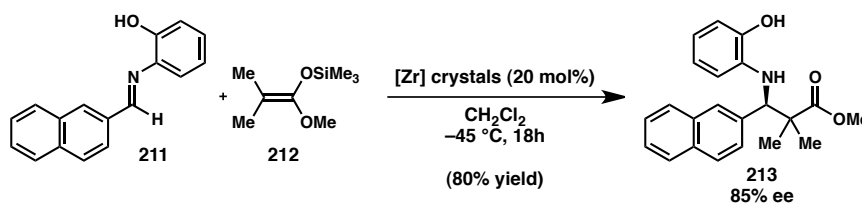


4.2.2 Reactions Promoted by Zirconium•BINOL Complexes

Chiral complexes of BINOL and zirconium have been used as Lewis acids to promote a variety of asymmetric reactions. These catalysts are generally prepared in situ from a zirconium alkoxide, resulting in a BINOLate complex. In contrast, the active catalyst in our conjugate addition/Prins cyclization contains a protonated BINOL ligand, allowing it to effect an asymmetric enolate protonation.

Chiral zirconium Lewis acids are most commonly used to activate carbonyls or imines in Strecker,⁷ Mannich,⁸ aldol,⁹ aldehyde allylation,¹⁰ and cycloaddition reactions.¹¹ The Kobayashi laboratory has developed an isolable zirconium catalyst for asymmetric Mannich reactions.^{8c} Addition of hexanes to a dichloromethane solution of a zirconium alkoxide, (*R*)-6,6'-dibromo-BINOL, and *N*-methylimidazole (NMI) causes precipitation of a white powder that is a stable (over at least 6 months) but highly active catalyst (Figure 8).

Figure 8. Asymmetric Mannich reaction promoted by isolable Zr catalyst.



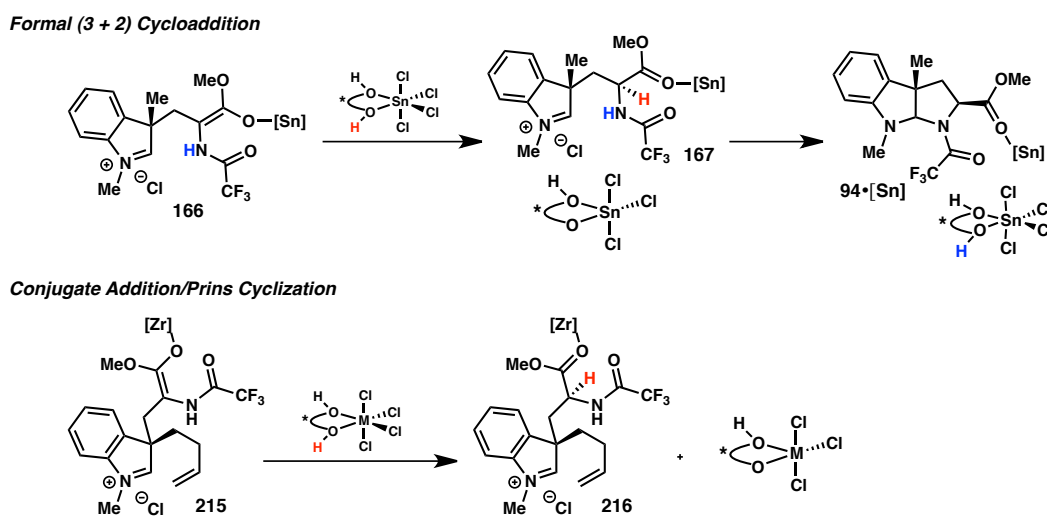
Recrystallization with *N*-benzylimidazole instead of NMI yielded single crystals suitable for X-ray crystallographic analysis. The X-ray structure showed a $\text{Zr}_4(\mu\text{-BINOLate})_6(\mu_3\text{-OH})_4$ complex (**214**), with four hexa-coordinated zirconium atoms and

six BINOL ligands. This represents the first X-ray crystallographic structure of a chiral zirconium-BINOL complex that is catalytically competent in Mannich-type reactions. To the best of our knowledge, there are no examples of zirconium complexes acting as chiral protonation catalysts prior to the development of our conjugate addition-Prins cyclization.

4.2.3 Investigation of Additives

Unfortunately, our initial efforts to improve the yield of the conjugate addition/asymmetric protonation/Prins cyclization by modifying the catalyst structure proved unfruitful. At this point, it was observed that the yield was correlated to catalyst loading, suggesting poor turnover of the deprotonated BINOLate.

Figure 9. Stoichiometric proton source.



One potential problem was the lack of a stoichiometric proton source to turn over the deprotonated BINOLate. In our previously studied pyrroloindoline formation, the

stoichiometric proton is likely provided by the pendant amide (Figure 9). While the full mechanistic picture of the formal (3 + 2) cycloaddition is likely more complicated than direct proton transfer from the amide to the BINOLate (as cyclization and thus amide deprotonation does not occur until work-up), we nonetheless hypothesized that a stoichiometric proton source might improve the yield of the Prins cyclization.

With this hypothesis in mind, the Prins reaction was performed with 1.6 equivalents of (*R*)-BINOL and 1.6 equivalents of ZrCl_4 . Unfortunately, the product was isolated in only 36% yield (Figure 10). Tentatively, this result can be explained by the fact that the (*R*)-BINOL• ZrCl_4 complex (Figure 10, inset) is too sterically hindered to effectively activate the acrylate substrate. It may be crucial to have free ZrCl_4 in solution to coordinate to the acrylate, in addition to (*R*)-BINOL• ZrCl_4 , which effects enolate protonation. Therefore, our next strategy to improve the yield of this transformation was to incorporate an external achiral, stoichiometric proton source to regenerate the BINOL catalyst.

Figure 10. Stoichiometric ligand.

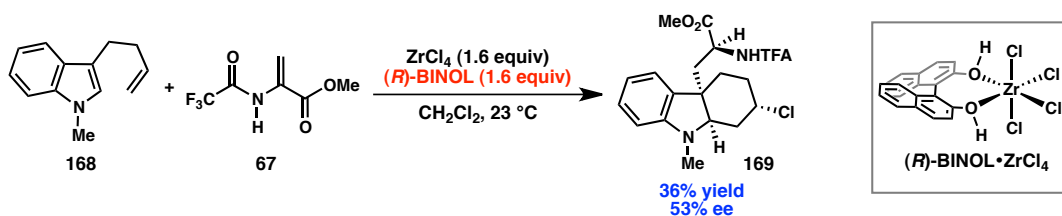
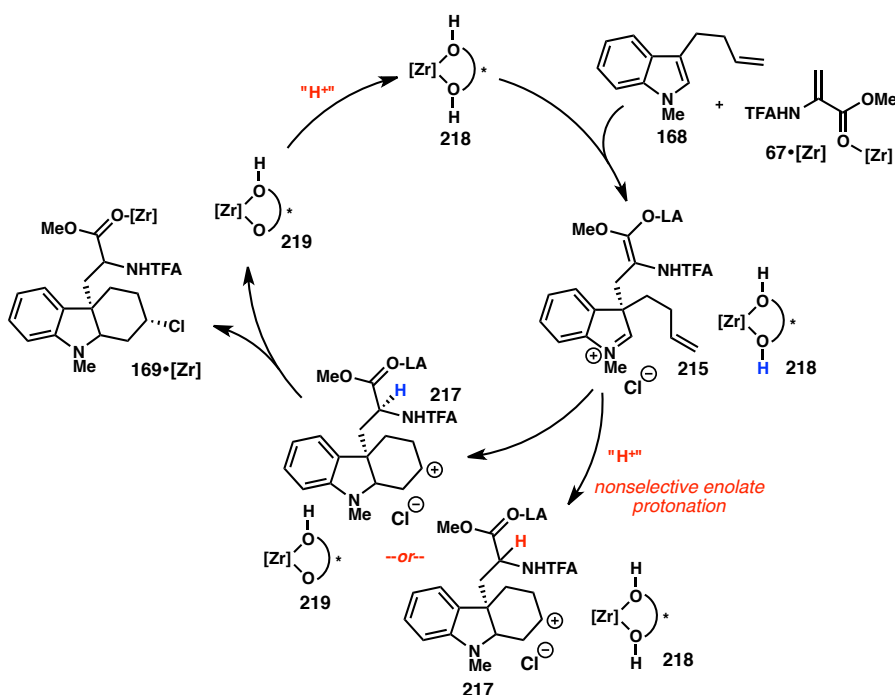


Figure 11 shows the desired reprotonation of the BINOLate by an external proton source (complex **219** → **218**). The rate of this reaction must be high enough to generate an adequate concentration of the active catalyst for protonation of the enolate. However,

this reagent may also participate in the nonselective direct protonation of enolate **215**, which would lower the ee of the product.

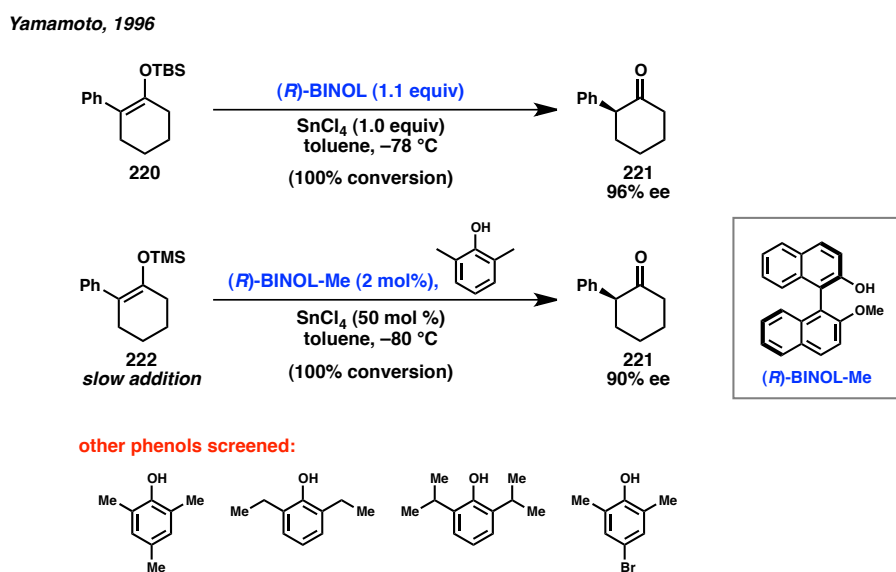
Figure 11. Incorporation of stoichiometric, achiral proton source.



Several strategies have been employed to turn over a chiral acid catalyst with a stoichiometric achiral proton source. Yamamoto and coworkers effected the enantioselective protonation of silyl enol ethers with the Lewis acid-assisted Brønsted acid (*R*)-BINOL-Me•SnCl₄ (Figure 12). The catalytic variant of this reaction utilizes 2,6-dimethylphenol as the stoichiometric proton source.¹² In this case, the silyl enol ether (**222**) was added slowly to the reaction in order to minimize its concentration in solution and ensure that it reacts with the catalyst rather than the phenol•SnCl₄ complex. The

achiral proton source was also carefully optimized after screening of several substituted phenols.

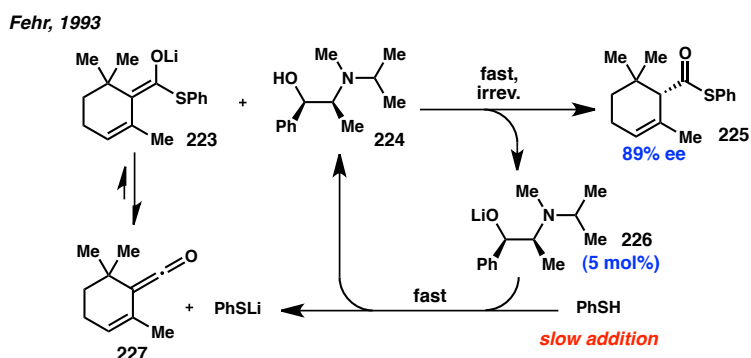
Figure 12. Catalytic enantioselective protonation of silyl enol ethers.



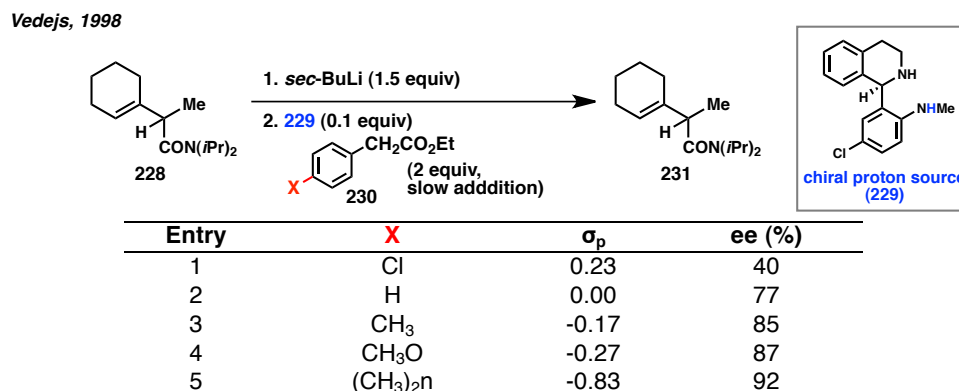
An early example of a catalytic enantioselective protonation of enolates was reported by Fehr and coworkers (Figure 13).¹³ In this transformation, the aromatic thiol serves as both nucleophile and stoichiometric proton source in the presence of a catalytic amount of lithiated *N*-isopropylephedrine (**226**). The thiol is added slowly to the reaction to avoid accumulation. It is then deprotonated by the ephedrine-derived base to generate thiophenoxide and the chiral proton source *N*-isopropylephedrine (**224**). Addition of the thiophenoxide to ketene **227** forms enolate **223**, which is rapidly and irreversibly protonated by *N*-isopropylephedrine (**224**) to give thioester **225** and regenerate the lithium base **226**. Thus, high enantioselectivity is achieved in this reaction by slowly

generating the enolate substrate in situ. The concentration of the stoichiometric proton source is also minimized by slow addition.

Figure 13. Catalytic enantioselective protonation of enolates.



Vedejs and Kruger undertook a systematic optimization of the $\text{p}K_{\text{a}}$ of the stoichiometric proton source in a catalytic, enantioselective protonation reaction (Table 3).¹⁴ The enantioselective protonation of the amide enolate derived from **228** was effected by chiral acid **229**. Their investigation utilized a series of substituted ethyl phenylacetate derivatives (**230**) with $\text{p}K_{\text{a}}$ values spanning 22–28 (DMSO). The enantioselectivities were found to increase with the electron-donating ability of the substituent X. As the acidity of the achiral proton source increases, nonselective protonation becomes competitive, leading to lower ee's. While this reaction was performed in THF as the solvent, the literature $\text{p}K_{\text{a}}$ values were determined in DMSO, so further comparisons between the $\text{p}K_{\text{a}}$ values of the substrate and achiral acid should be regarded with caution.

Table 3. pK_a of achiral acid vs. enantioselectivity.

Based on these precedents, the use of additives in the conjugate addition/Prins cyclization was investigated. Initially, various substituted phenols were added as stoichiometric proton sources. The phenol would need to be carefully optimized to minimize the rate of nonselective protonation of the enolate. While 2,6-dimethylphenol provided a boost in yield, the ee was also lower (Table 4, entry 2), indicating that nonselective enolate protonation by the achiral phenol is occurring. On the other hand, use of the more hindered 2,6-*t*-Bu₂-phenol failed to improve the yield (entry 3), i.e., the rate of proton transfer from the phenol to the BINOLate is too low.

In an attempt to reduce nonselective enolate protonation by 2,6-dimethylphenol, the indole substrate was added slowly over the course of the reaction to reduce the concentration of enolate (entry 4). Unfortunately, this only served to reduce the rate of reaction; the product was isolated in only 34% yield. As an alternative strategy to reduce the rate of nonselective protonation, various phenols were then added slowly over the course of reaction. Use of 2,6-dimethylphenol did not aid in catalyst turnover (entry 5). The less sterically hindered unsubstituted phenol and more acidic 4-bromophenol also failed to improve the yield of **169** (entries 6, 7).

Table 4. Screen of achiral proton sources.

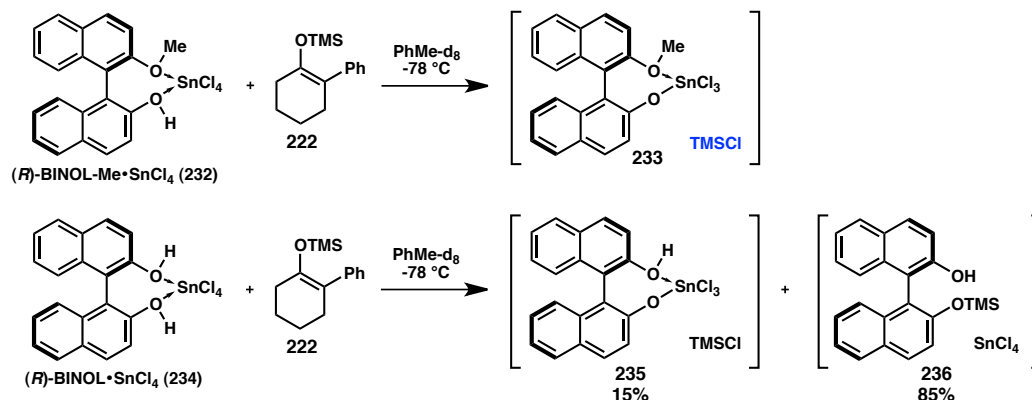
Entry	Achiral H ⁺ Source	Yield (%)	ee (%)
1	--	30	40
2	2,6-dimethylphenol	66	19
3	2,6-di- <i>t</i> -butylphenol	34	45
4 ^a	2,6-dimethylphenol	23	26
5 ^b	2,6-dimethylphenol	27	37
6 ^b	phenol	33	35
7 ^b	4-bromophenol	35	24

^a slow addition of indole. ^b slow addition of achiral proton source.

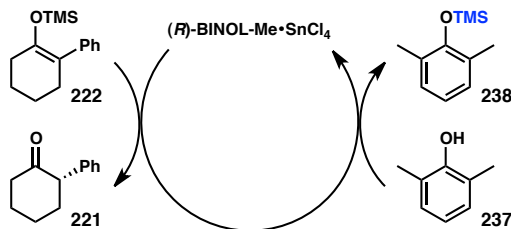
NMR studies of Yamamoto's asymmetric protonation of silyl enol ethers promoted by *stoichiometric* (*R*)-BINOL-Me•SnCl₄ revealed formation of a tin-aryloxide species (**233**) and TMSCl (Figure 14a).¹² On the other hand, reaction with the unmethylated (*R*)-BINOL resulted in formation of the inactive silylated diol **236**. The former complex was found to be a more effective catalyst. They proposed that in the catalytic reaction employing 2,6-dimethylphenol as the stoichiometric proton source, the tin complex receives a proton and chloride from the phenol and TMSCl, respectively, and TMS-2,6-dimethylphenol is formed as a byproduct (Figure 14b). It was hypothesized in our Prins cyclization, a Lewis acid complex such as **239** is formed after donation of a proton to the enolate and a chloride to quench the carbocation. Proton transfer from a phenol to complex **239** may be unfavorable, but further addition of a chloride source such as TMSCl may aid in regenerating the active BINOL•ZrCl₄ complex (**241**, Figure 14c).

Figure 14. (a) Yamamoto's NMR studies of LBA-promoted enantioselective silyl enol ether protonation. (b) Yamamoto's catalytic enantioselective silyl enol ether protonation. (c) Hypothesis for promoting catalyst turnover in the conjugate addition/Prins cyclization.

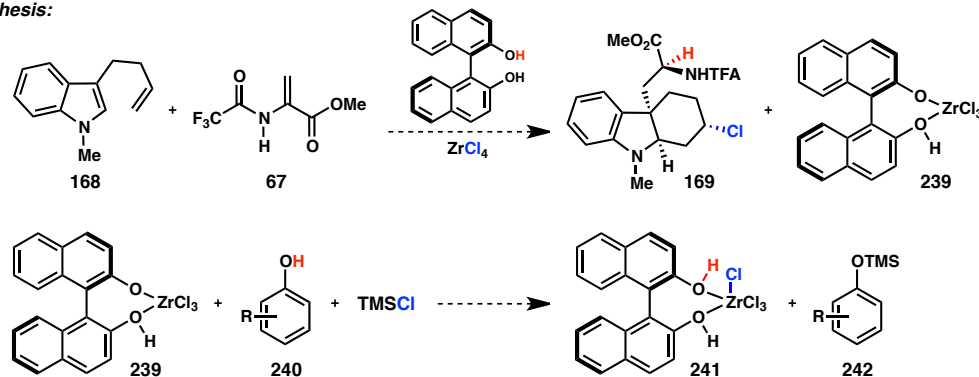
a. Stoichiometric reaction:



b. Catalytic reaction:



c. Hypothesis:



With this hypothesis in mind, the Prins reaction was performed in the presence of 1.0 equivalent of TMSCl and 1.0 equivalent of 2,6-dimethylphenol. Gratifyingly, the product **169** was isolated in 71% yield (Table 5, entry 1). Methylation of the catalyst resulted in a slight improvement in yield and ee (entry 2). Functionalization of the diol

with a benzoyl group, which is capable of coordinating to the Lewis acid, was highly detrimental to enantioselectivity (entry 4). Catalysts substituted with bromines at the 3 and 3' positions were also screened. Surprisingly, the relationship between ee and the alkyl group (entries 5-7) was inconsistent with the analogous trend for backbone-unsubstituted catalysts (entries 1-3).

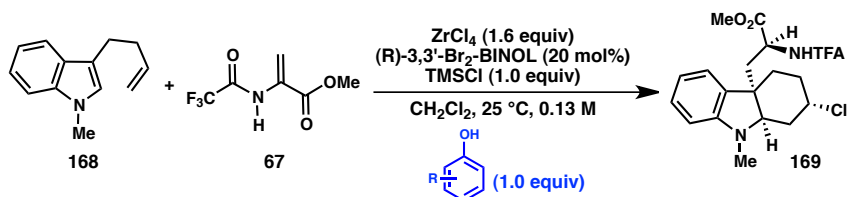
Table 5. Screen of alkylated BINOL derivatives incorporating TMSCl.

Entry	Catalyst	Yield (%)	ee (%)
1	(<i>R</i>)-BINOL	71	28
2	(<i>R</i>)-BINOL-Me	81	46
3	(<i>R</i>)-BINOL-Bn	90	31
4	(<i>R</i>)-BINOL-Bz	84	2
5	(<i>R</i>)-3,3'-Br ₂ -BINOL	72	50
6	(<i>R</i>)-3,3'-Br ₂ -BINOL-Me	70	12
7	(<i>R</i>)-3,3'-Br ₂ -BINOL-Bn	80	60

Since (*R*)-3,3'-Br₂-BINOL-Bn did not provide a significant increase in enantioselectivity compared to (*R*)-3,3'-Br₂-BINOL, most of the subsequent screening was performed with the unalkylated catalyst due to ease of preparation.

To investigate the possibility of cooperative effects between the chiral diol and the achiral, stoichiometric proton donor, a variety of phenol derivatives were screened. The rate of nonselective enolate protonation was expected to be related to the electronic and steric profile of the achiral proton source (Table 6). 3,5-Dimethoxyphenol was found to give unexpectedly high ee, albeit in only 40% yield (entry 7), while 2,6-dimethoxyphenol was less successful (entry 6).

Table 6. Screen of phenol derivatives.



Entry	Phenol Substitution	Yield (%)	ee (%)
1	2-Me	72	21
2	2,6-Me ₂	72	50
3	2-OMe	52	7
4	3-OMe	47	21
5	4-OMe	66	20
6	2,6-(OMe) ₂	36	16
7	3,5-(OMe) ₂	40	86
8	2-F	63	52
9	2-Cl	78	80
10 ^a	2-Cl	72	17
11 ^b	2-Cl	71	65
12	2-Br	79	66
13	3-Cl	76	50
14	4-Cl	67	26
15	2,6-F ₂	70	67
16	2,4-Cl ₂	80	63
17	2,6-Cl ₂	71	87
18 ^c	2,6-Cl ₂	66	86
19 ^d	2,6-Cl ₂	74	83
20 ^e	2,6-Cl ₂	68	87
21 ^f	2,6-Cl ₂	67	87
22 ^g	2,6-Cl ₂	77	87
23	2,6-Cl ₂ -4-Me	84	87
24	2,4,6-Cl ₃	77	86
25	2,6-Br ₂	56	86

^a (R)-3,3'-Br₂-BINOL-Me was used as the catalyst. ^b (R)-3,3'-Br₂-BINOL-Bn was used as the catalyst. ^c TESCOl (1.0 equiv) instead of TMSCl. ^d [indole] = 0.2 M. ^e [indole] = 0.1 M. ^f Reaction run at 40 °C. ^g Reaction run in DCE.

Keeping in mind that the methoxy group is electron-withdrawing in the *meta* position (as reflected by its Hammett substituent constant σ_m), halogenated phenols were screened next. Of the *ortho*-monosubstituted phenols, 2-chlorophenol gave the best results. Interestingly, the alkylated catalysts (R)-3,3'-Br₂-BINOL-Me (entry 10) and (R)-3,3'-Br₂-BINOL-Bn (entry 11) in conjunction with 2-chlorophenol resulted in lower ee, in contrast to the trend observed with 2,6-dimethylphenol. Finally, *ortho*-dichlorinated

phenols were found to provide both good yields and ee's (entries 16-24); the optimal phenol also incorporates a slightly electron-donating *para*-methyl group (entry 23).

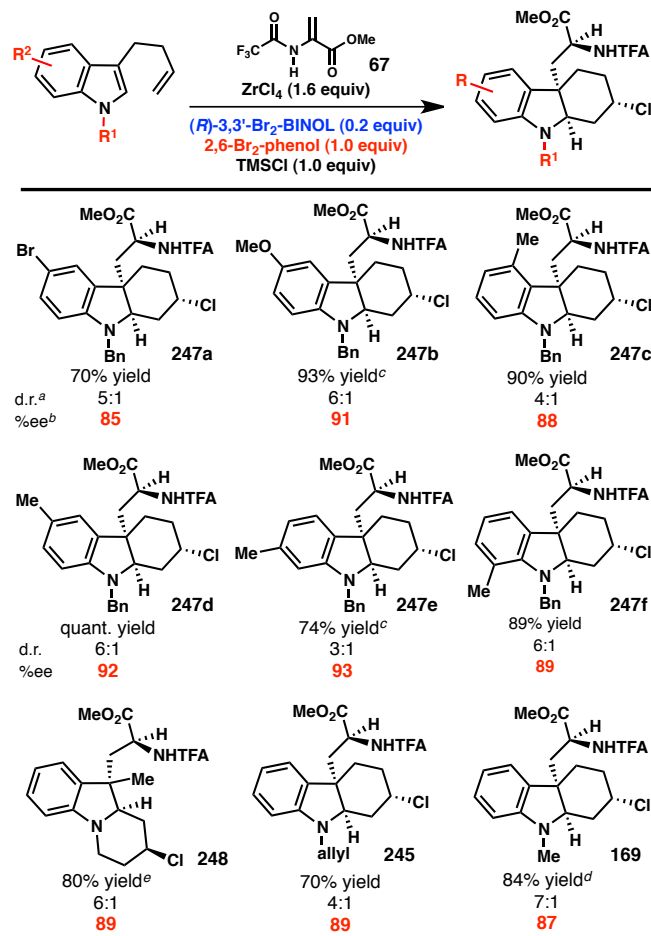
Indole substrates protected with either allyl or benzyl groups were then investigated (Table 7). Unfortunately, the optimal stoichiometric proton source (2,6-dichloro-4-methylphenol) for the reaction with *N*-methylindoles was not optimal for these alternative substrates, reflecting the delicate balance of reaction rates required to achieve good yield and enantioselectivity in this transformation. For both *N*-allyl- and *N*-benzylindoles, 2,6-dibromophenol was chosen as the optimal proton source because it is commercially available and also provides good yields and ee's.

Table 7. Screen of indole protecting groups.

Entry	Protecting Group	Phenol Substitution	Yield (%)	ee (%)
1	allyl	2,6-Cl ₂	70	87
2	allyl	2,6-Cl ₂ -4-Me	75	86
3	allyl	2,4,6-Cl ₃	79	83
4	allyl	2,6-Br ₂	70	90
5	allyl	2,6-Br ₂ -4-Me	71	87
6	allyl	2,4,6-Br ₃	52	84
7	Bn	2,6-Cl ₂ -4-Me	74	85
8	Bn	2,6-Br ₂	82	91
9	Bn	2,6-Br ₂ -4-Me	67	91
10	Bn	2,6-Br ₂ -4-OMe	77	84
11	Bn	2,6-Br ₂ -4- <i>t</i> Bu	78	90
12	Bn	2,4,6-Br ₃	76	86

4.2.4 Substrate Scope of the Conjugate Addition/Prins Cyclization

Table 8. Substrate scope.



^a Determined by ^1H NMR of crude reaction mixture. ^b Determined by SFC using chiral stationary phase. ^c 1.1 equiv. ZrCl_4 was employed. ^d 2,6-dichloro-4-methylphenol was employed. ^e 2,6-dibromo-4-*t*-butylphenol was employed.

Having identified optimal reaction parameters, a screen of indole substrates was conducted. For the 5-bromoindole substrate, the *N*-Me protecting group (to yield **247**) gave improved enantioselectivity over *N*-Bn. The benzyl group was utilized for the other substrates with indole backbone substitution. Surprisingly, both 5-methoxy- and 6-methyl-substituted substrates, when exposed to the standard reaction conditions, yielded a significant quantity of the corresponding pyrroloindoline. It is possible that the electron-

donating property of the methoxy substituent decreases the electrophilicity of the indolinium ion, thus disfavoring addition by the tethered alkene. Upon work-up, the unreacted indolinium ion is attacked by the pendant amide to give the pyrroloindoline. It is unclear why Prins cyclization is disfavored in the case of the 6-methyl-substituted substrate. Fortunately, yields of both Prins products (**246b** and **246e**) were improved by reducing the amount of ZrCl_4 to 1.1 equivalents.

We were pleased to find that *N*-homoallylindole smoothly underwent conjugate addition and Prins cyclization. However, under the standard reaction conditions, the product (**248**) was isolated in only 86% ee (Table 9). A screen of substituted phenols revealed 2,6-dibromo-4-*t*-butylphenol to be optimal, giving the product in 89% ee and 80% yield (entry 6).

Table 9. Screen of phenol additives to *N*-tethered substrate.

Entry	Phenol Substitution	Yield (%) ^a	ee (%)
1	2,6-Cl ₂	82	86
2	2,4,6-Cl ₃	(62)	85
3	2,6-Cl ₂ -4-Me	(76)	84
4	2,6-Br ₂	80	86
5	2,4,6-Br ₃	84	87
6	2,6-Br ₂ -4- <i>t</i> Bu	80	89

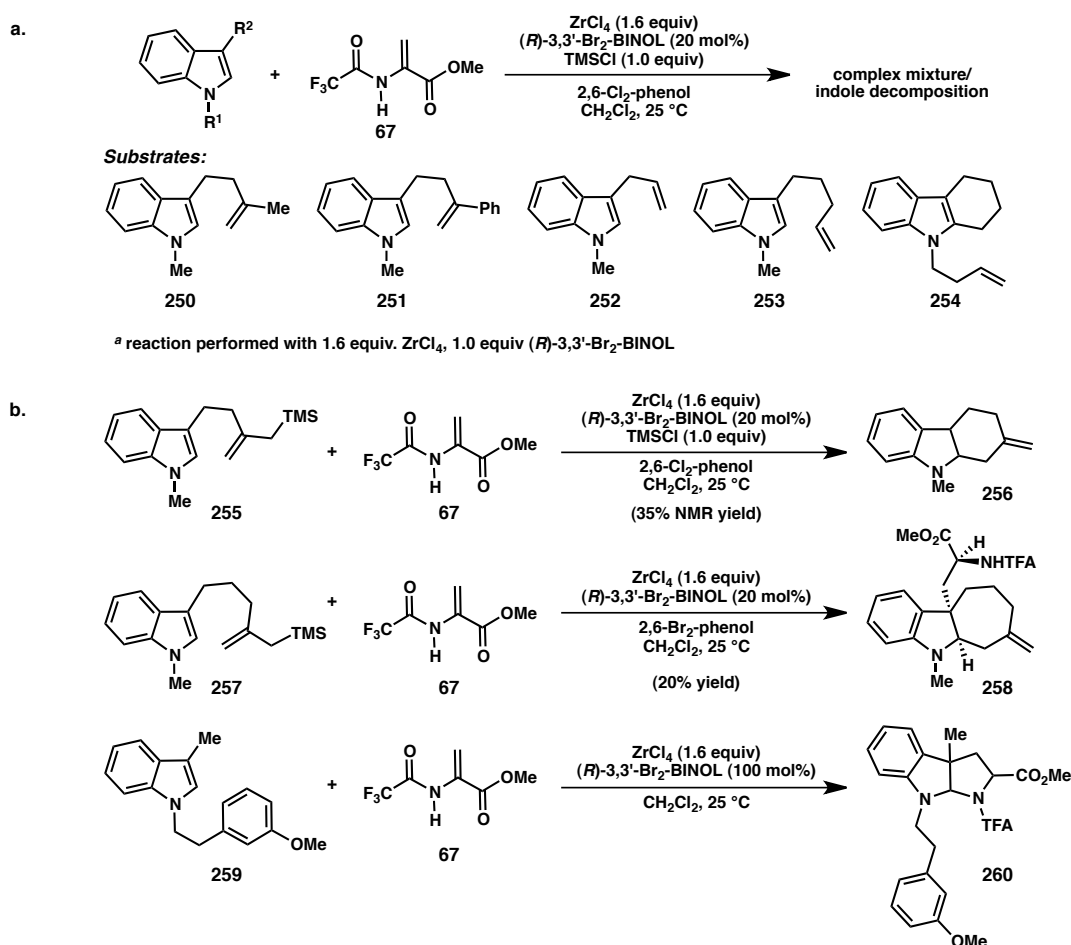
^a Yields in parentheses are determined by integration of crude ¹H NMR with respect to (R)-3,3'-Br₂-BINOL. Other yields are isolated.

4.2.5 Unsuccessful Substrates

Several substrates with alternative tether structures were synthesized. When exposed to the conditions for the conjugate addition/Prins cyclization, many formed

complex mixtures of products (Figure 15a). However, some substrates underwent competing reaction mechanisms. For example, the allylsilane moiety of indole **255** facilitates cyclization such that it occurs at a faster rate than conjugate addition, and the observed product results from protonation of the indole followed by cyclization. On the other hand, a small amount of the desired product was formed from allylsilane substrate **257**, likely because cyclization to form the seven-membered ring is slower than the six-membered ring analogue (**258** vs. **256**). Friedel–Crafts substrate **259** failed to undergo cyclization by the aryl ring, forming the pyrroloindoline instead.

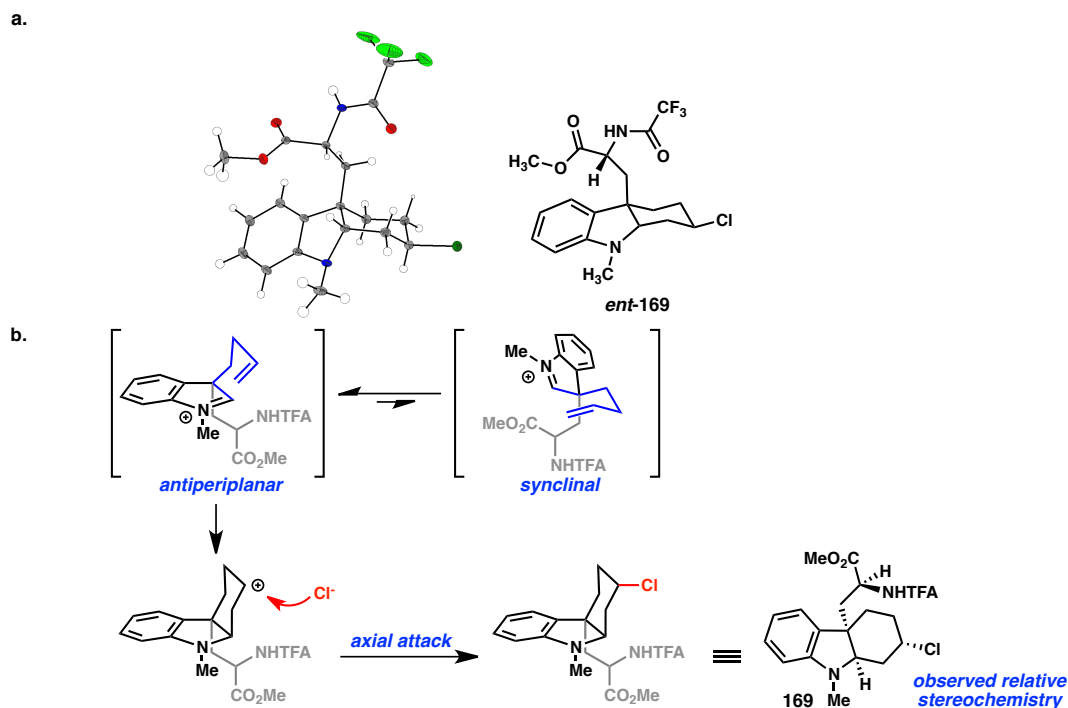
Figure 15. Unsuccessful alternative substrates.



4.2.6 Mechanistic Considerations

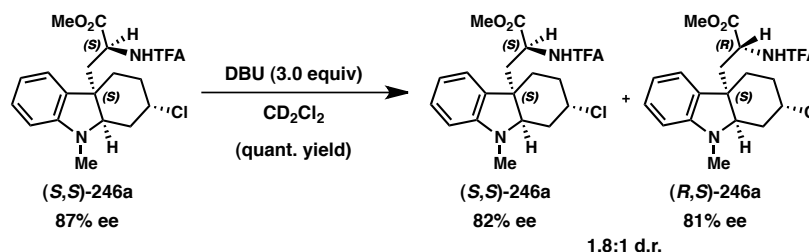
The relative stereochemistry of the major diastereomer of conjugate addition/Prins cyclization product **169** was determined by single crystal X-ray crystallography (Figure 16, crystal structure shows enantiomer). Aza-Prins cyclizations which form six-membered rings favor transition states with an antiperiplanar alignment of the iminium ion and alkene, rather than a synclinal arrangement, because overlap between the alkenyl π -system and the developing lone pair on nitrogen is maximized.¹⁵ In this case, the observed chloride stereochemistry results from axial attack, which is generally disfavored in intermolecular cases. Alternatively, chloride delivery may occur in an intramolecular fashion from a zirconium species coordinated to the ester or amide carbonyl, or the carbocation intermediate can chair flip prior to chloride attack.

Figure 16. Relative stereochemistry of conjugate addition/Prins products.



The major product of the conjugate addition/Prins cyclization is the (*S,S*) diastereomer (absolute stereochemistry determined by analogy to the pyrroloindoline synthesis). Epimerization of diastereomerically pure Prins product (*S,S*)-**246a** returns a mixture of (*S,S*)-**246a** and (*R,S*)-**246a**, where (*R,S*)-**246a** is the enantiomer of the minor diastereomer formed in the Prins reaction (Figure 17). Thus, the originally-formed diastereomers (*S,S*)-**246a** and (*S,R*)-**246a** have opposite configurations at the quaternary center, which is consistent with the (*R*)-3,3'-dibromo-BINOL•ZrCl₄ complex acting as an asymmetric protonation catalyst in an analogous fashion to the (*R*)-BINOL•SnCl₄ complex. Furthermore, the configuration of the chloride is linked to the stereochemistry of the C3 quaternary center.

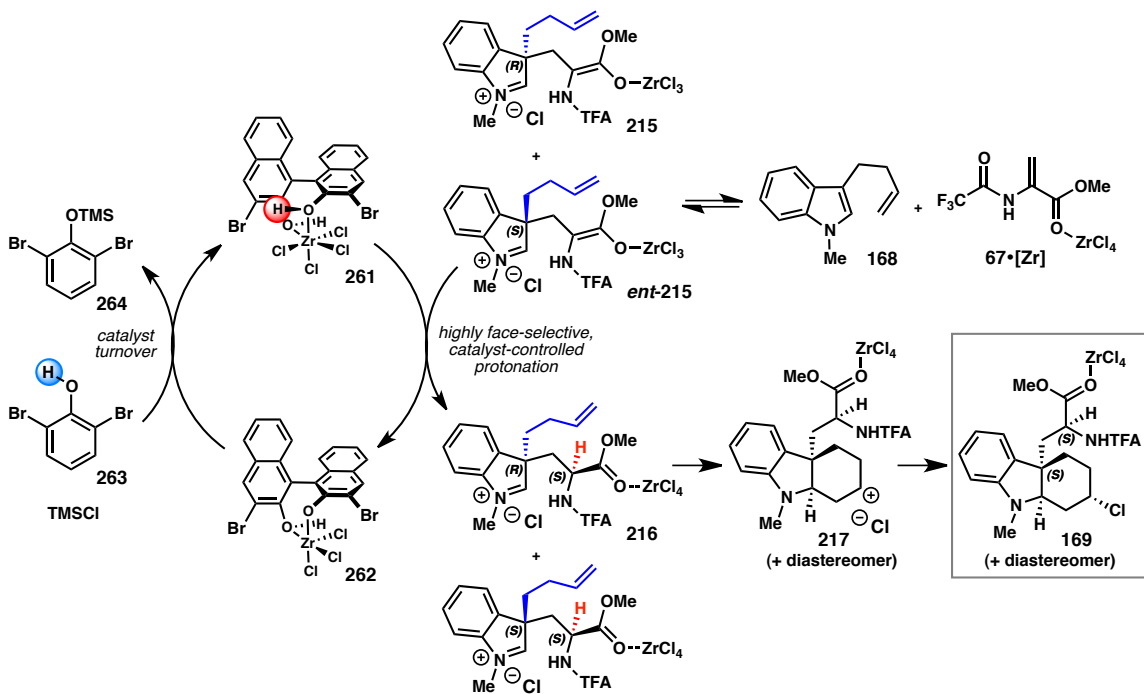
Figure 17. Epimerization study.



A possible mechanism of the conjugate addition/Prins cyclization is proposed in Figure 18. Activation of the acrylate (**67**) by a zirconium Lewis acid facilitates conjugate addition by the indole (**168**) to afford enantiomeric enolate intermediates (**215** and *ent*-**215**). Next, catalyst-controlled, face-selective enolate protonation occurs to yield iminium ions **216**. These first steps are analogous to the formal (3 + 2) cycloaddition to prepare pyrroloindolines. However, in the Prins reaction, the presence of a tethered alkene leads to intramolecular cyclization (to give **217**) followed by chloride quenching of the

resulting carbocation (to yield **169**). The (*R*)-3,3'-Br₂-BINOLate•ZrCl₄ complex (**262**) receives a chloride from TMSCl and a proton from the achiral phenol (**263**) to regenerate the active protonation catalyst (**261**).

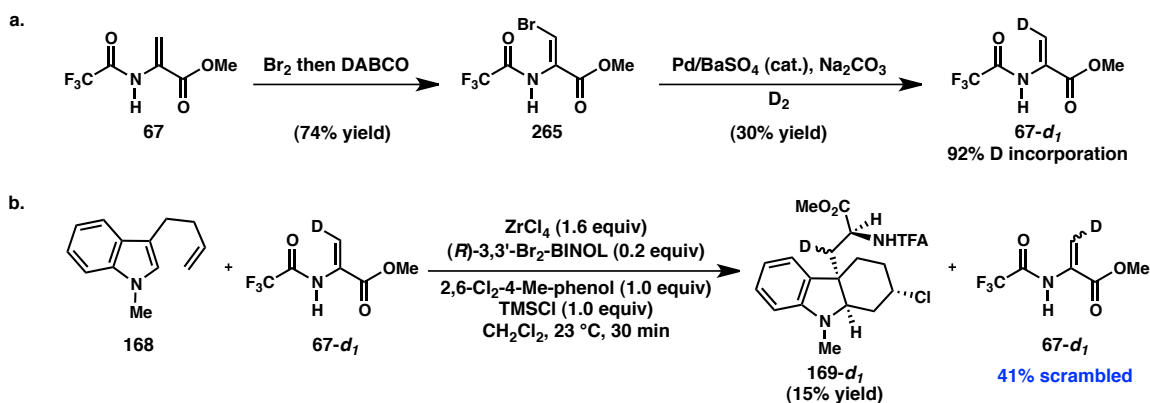
Figure 18. Proposed mechanism of the conjugate addition/Prins cyclization.



In this proposed mechanism, the initial conjugate addition step may be catalyzed by ZrCl₄ rather than (*R*)-3,3'-Br₂-BINOL•ZrCl₄, and thus is not stereoselective. However, the reversability of conjugate addition, coupled with the difference in protonation rates arising from matching/mismatching of the enantiomeric enolates with the chiral catalyst, leads to the observed diastereoselectivity. To probe the reversability of the conjugate addition step, a stereodefined deuterated acrylate (**67-d₁**) was synthesized (Figure 19a). Stereochemical information about the acrylate alkene is lost upon conjugate addition; if

this step is reversible, then the deuterium label should undergo scrambling. However, if conjugate addition is not reversible, no scrambling would be expected. When this acrylate was subjected to the Prins reaction conditions (run to low conversion), significant scrambling of the deuterium label was observed in the reisolated acrylate (Figure 19b, 41% had opposite alkene stereochemistry compared to starting acrylate). A control reaction performed in the absence of the indole substrate showed no deuterium scrambling. This result is consistent with a reversible conjugate addition step.

Figure 19. Stereochemical probe of reversability of conjugate addition.

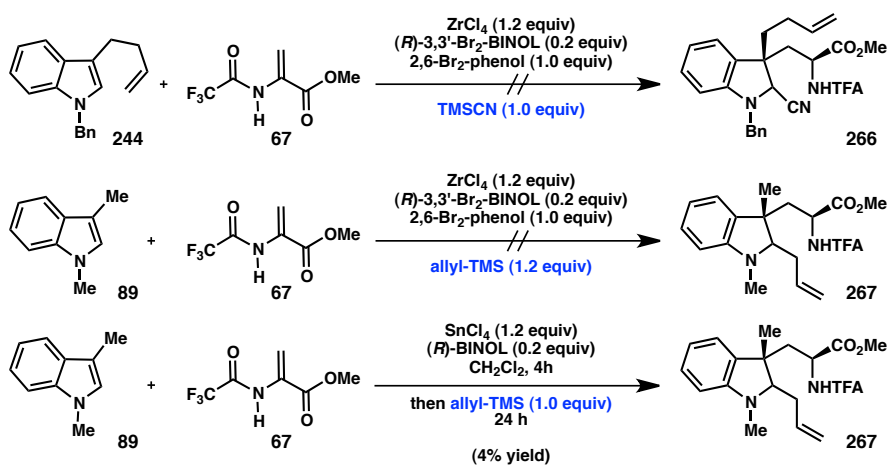


4.2.7 Extension to Intermolecular Nucleophiles

Preliminary investigations into extending this methodology to intermolecular carbon nucleophiles have been performed (Figure 20). When 3-homoallyl indole **244** was exposed to the conjugate addition/Prins cyclization conditions with TMSCN as an external nucleophile, the intermolecular trapping product was not formed. Instead, the major product observed was the Prins cyclization product. However, using SnCl_4 as the

Lewis acid and allyltrimethylsilane as the nucleophile gave a small amount of the C2-allylated product (**267**). Development of this methodology will likely require further screening of Lewis acids.

Figure 20. Preliminary investigation of intermolecular nucleophiles.



4.3 Concluding Remarks

We have developed a novel conjugate addition/Prins cyclization for the synthesis of enantioenriched fused indolines. This reaction is based on the observation that the formal (3 + 2) cycloaddition to prepare pyrroloindolines from 3-substituted indoles and 2-amidoacrylates forms an iminium ion as the initial product, and cyclization to the pyrroloindoline does not occur until aqueous work-up. Attempts to trap this iminium ion with alternative nucleophiles led us to design an indole substrate with a tethered alkene. This alkene undergoes an intramolecular Prins cyclization, while a chloride ion from the Lewis acid traps the resulting carbocation.

A screen of Lewis acids revealed ZrCl_4 to be optimal, while (*R*)-3,3'-dibromo-BINOL gave the best combination of yield and enantioselectivity. The (*R*)-3,3'- Br_2 -BINOL• ZrCl_4 complex acts as an asymmetric protonation catalyst in an analogous fashion to the (*R*)-BINOL• SnCl_4 catalyst utilized in the pyrroloindoline synthesis. Additives were found to be necessary to achieve catalyst turnover in this transformation. After the (*R*)-3,3'- Br_2 -BINOL• ZrCl_4 complex effects enolate protonation and donates a chloride ion, it receives a proton from an achiral phenol and a chloride from TMSCl .

A stereodefined, deuterium-labelled acrylate substrate was designed as a probe for the reversability of the conjugate addition step. Results from this experiment are consistent with conjugate addition being reversible.

4.4 Experimental Section

4.4.1 Materials and Methods

Unless otherwise stated, reactions were performed under a nitrogen atmosphere using freshly dried solvents. Tetrahydrofuran, methylene chloride, toluene, and hexanes were dried by passing through activated alumina columns. Dimethylformamide was dried over activated molecular sieves, and dichloroethane was distilled over calcium hydride. Deuterated methylene chloride (CD_2Cl_2) for the experiments resubjecting the pyrroloindoline products to reaction conditions was dried by passing through a plug of activated alumina. All other commercially obtained reagents were used as received unless specifically indicated. EtAlCl_2 (neat) and 1 M SnCl_4 in DCM were purchased from Aldrich and (*R*)-BINOL was obtained from Alfa Aesar. Reactions were monitored by thin-layer chromatography using EMD/Merck silica gel 60 F254 pre-coated plates (0.25 mm) and were visualized by UV, *p*-anisaldehyde, or KMnO_4 staining. Flash column chromatography was performed either as described by Still et al. using silica gel (particle size 0.032-0.063) purchased from Silicycle, or pre-packaged RediSep[®]Rf columns on a CombiFlash Rf system (Teledyne ISCO Inc.). Diastereomeric ratios were determined by integration of NMR spectra or HPLC or SFC analysis. Optical rotations were measured on a Jasco P-2000 polarimeter using a 100 mm path-length cell at 589 nm. ^1H and ^{13}C NMR spectra were recorded on a Varian Mercury 300 (at 300 MHz and 75 MHz, respectively), a Varian 400 (at 400 MHz and 100 MHz, respectively) or a Varian Inova 500 (at 500 MHz and 125 MHz, respectively), and are reported relative to internal chloroform (^1H , $\delta = 7.26$, ^{13}C , $\delta = 77.0$). Data for ^1H NMR spectra are reported as follows: chemical shift (δ ppm) (multiplicity, coupling constant (Hz), integration).

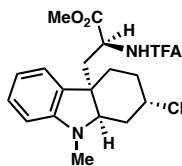
Multiplicity and qualifier abbreviations are as follows: s = singlet, d = doublet, t = triplet, q = quartet, m = multiplet, br = broad, app = apparent. IR spectra were recorded on a Perkin Elmer Paragon 1000 spectrometer and are reported in frequency of absorption (cm^{-1}). Preparative HPLC was performed with either an Agilent 1100 or 1200 Series HPLC utilizing an Agilent Zorbax RX-SIL $5\mu\text{m}$ column (9.4 x 250 mm). Analytical chiral HPLC was performed with an Agilent 1100 Series HPLC utilizing Chiralcel AD or OD-H columns (4.6 mm x 25 cm) obtained from Daicel Chemical Industries, Ltd with visualization at 254 nm. Analytical SFC was performed with a Mettler SFC supercritical CO_2 analytical chromatography system with Chiralcel AD-H and OJ-H columns (4.6 mm x 25 cm). Melting points were determined using a Büchi B-545 capillary melting point apparatus and the values reported are uncorrected. HRMS were acquired using either an Agilent 6200 Series TOF with an Agilent G1978A Multimode source in electrospray ionization (ESI), atmospheric pressure chemical ionization (APCI) or mixed (MM) ionization mode, or obtained from the Caltech Mass Spectral Facility.

4.4.2 General Procedure A. Conjugate Addition/Asymmetric Protonation/Prins Cyclization Cascade

To a flame-dried flask was added indole (0.20 mmol, 1.00 equiv), acrylate (0.24 mmol, 1.20 equiv), and (*R*)-3,3'-dibromo-BINOL (0.04 mmol, 0.20 equiv), and phenol (0.20 mmol, 1.00 equiv). The flask was charged with DCM (1.5 mL), followed by addition of TMSCl (0.2 mmol, 1.00 equiv), ZrCl₄ (0.32 mmol, 1.60 equiv unless specifically indicated), then stirred at room temperature for 24 h. The reaction was quenched by diluting with 1 mL MeCN and 1 mL 1 M HCl, followed by addition of 5 mL H₂O. The aqueous layer was extracted with ethyl acetate (3 x 5 mL) and the combined organic layers were washed with either saturated NaHCO_{3(aq)} (10 mL). The aqueous layer was back extracted with EtOAc (10 mL) and the combined organic layers were dried (Na₂SO₄), filtered, and concentrated. The crude residue was purified by flash chromatography.

4.4.3 Indoline Products from Conjugate Addition/Asymmetric Protonation/Prins Cyclization Cascade

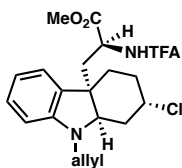
Indoline 169.



Prepared from 1-methyl-3-homoallyl-1*H*-indole and methyl 2-trifluoroacetamidoacrylate using General Procedure A to yield **169** in 84% yield. The diastereomeric ratio was determined to be 7:1 by ¹H NMR analysis of the crude reaction mixture. The enantiomeric excess of the major diastereomer was determined to be 87% by chiral SFC

analysis (AD-H, 2.5 mL/min, 7% IPA in CO₂, λ = 254 nm): t_R (major) = 4.9 min; t_R (minor) = 6.0 min. The major diastereomer was separated by flash chromatography (10% ethyl acetate/hexanes). ¹H NMR (500 MHz, CDCl₃) δ 7.14 (td, J = 7.7, 1.3 Hz, 1H), 6.95 (dd, J = 7.3, 0.8 Hz, 1H), 6.82 (d, J = 7.8 Hz, 1H), 6.75 (td, J = 7.4, 0.9 Hz, 1H), 6.54 (d, J = 7.8 Hz, 1H), 4.55 (td, J = 7.6, 5.8 Hz, 1H), 4.28 – 4.21 (m, 1H), 3.50 (s, 3H), 3.45 (t, J = 5.1 Hz, 1H), 2.72 (s, 3H), 2.41 (dd, J = 14.9, 7.4 Hz, 1H), 2.24 (dd, J = 14.9, 5.7 Hz, 1H), 2.13 – 1.99 (m, 2H), 1.91 – 1.76 (m, 4H); ¹³C NMR (126 MHz, CDCl₃) δ 171.3, 156.5 (q, J_{C-F} = 37.7 Hz), 150.9, 133.0, 128.5, 121.7, 118.8, 115.5 (q, J_{C-F} = 287.6 Hz), 108.8, 68.7, 55.8, 52.6, 50.2, 44.5, 37.8, 32.9, 32.8, 32.0, 31.0; IR (NaCl/thin film) 3312, 2954, 2864, 1711, 1607, 1482, 1209, 1178 cm⁻¹; [α]_D²⁵ = +55.6 (c = 2.06, CH₂Cl₂). HRMS (MM) calc'd for C₁₉H₂₂ClF₃N₂O₃ [M+H]⁺ 419.1344, found 419.1358.

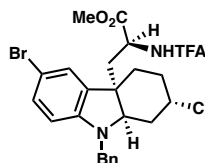
Indoline 245.



Prepared from 1-allyl-3-homoallyl-1*H*-indole and methyl 2-trifluoroacetamidoacrylate using General Procedure A to yield **245** in 70% yield. The diastereomeric ratio was determined to be 4:1 by ¹H NMR analysis of the crude reaction mixture. The enantiomeric excess of the major diastereomer was determined to be 89% by chiral SFC analysis (OD-H, 2.5 mL/min, 7% IPA in CO₂, λ = 254 nm): t_R (major) = 7.3 min; t_R (minor) = 4.9 min. The major diastereomer was separated by recrystallization (10% ethyl acetate/hexanes). ¹H NMR (500 MHz, CDCl₃) δ 7.11 (td, J = 7.7, 1.3 Hz, 1H), 6.94 (dd, J = 7.3, 0.8 Hz, 1H), 6.73 (td, J = 7.4, 0.9 Hz, 1H), 6.60 (d, J = 7.7 Hz, 1H), 6.57 (d,

$J = 7.8$ Hz, 1H), 5.87 (dddd, $J = 17.2, 10.2, 7.0, 4.8$ Hz, 1H), 5.31 (ddd, $J = 17.2, 3.1, 1.6$ Hz, 1H), 5.25 (ddd, $J = 10.2, 2.8, 1.4$ Hz, 1H), 4.62 (dd, $J = 13.8, 7.5$ Hz, 1H), 4.23 (qd, $J = 7.6, 3.7$ Hz, 1H), 3.91 (ddt, $J = 15.9, 4.8, 1.6$ Hz, 1H), 3.68 (t, $J = 4.9$ Hz, 1H), 3.64 – 3.56 (m, 1H), 3.47 (s, $J = 2.1$ Hz, 3H), 2.41 (dd, $J = 14.8, 7.3$ Hz, 1H), 2.27 (dd, $J = 14.8, 6.0$ Hz, 1H), 2.11 (dt, $J = 13.5, 4.1$ Hz, 1H), 2.03 – 1.94 (m, 1H), 1.93 – 1.73 (m, 4H); ^{13}C NMR (126 MHz, CDCl_3) δ 171.4, 156.4 (q, $J_{\text{C-F}} = 37.8$ Hz), 149.6, 133.2, 133.0, 128.4, 121.8, 118.6, 117.9, 115.4 (q, $J_{\text{C-F}} = 288.0$ Hz), 109.0, 65.8, 55.7, 52.6, 50.1, 48.2, 44.4, 37.33, 32.9, 32.2, 31.0; IR (NaCl/thin film) 3310, 2951, 1711, 1606, 1553, 1479, 1462, 1441, 1209, 1174 cm^{-1} ; $[\alpha]_{\text{D}}^{25} = 78.1$ ($c = 1.39$, CH_2Cl_2). HRMS (MM) calc'd for $\text{C}_{21}\text{H}_{23}\text{ClF}_3\text{N}_2\text{O}_3$ $[\text{M}+\text{H}]^+$ 445.1500, found 445.1496.

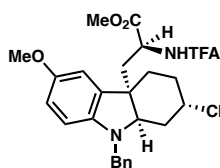
Indoline 247a.



Prepared from 1-benzyl-3-homoallyl-5-bromo-1*H*-indole and methyl 2-trifluoroacetamidoacrylate using General Procedure A to yield **247a** in 70% yield. The diastereomeric ratio was determined to be 5:1 by ^1H NMR analysis of the crude reaction mixture. The enantiomeric excess of the major diastereomer was determined to be 85% by chiral SFC analysis (OD-H, 2.5 mL/min, 10% EtOH in CO_2 , $\lambda = 254$ nm): t_{R} (major) = 9.5 min; t_{R} (minor) = 7.7 min. ^1H NMR (500 MHz, CDCl_3) δ 7.38 – 7.28 (m, 5H), 7.15 (dd, $J = 8.3, 2.0$ Hz, 1H), 7.03 (d, $J = 2.0$ Hz, 1H), 6.68 (d, $J = 8.1$ Hz, 1H), 6.36 (d, $J = 8.4$ Hz, 1H), 4.62 (dd, $J = 14.6, 6.6$ Hz, 1H), 4.38 (d, $J = 15.6$ Hz, 1H), 4.22 – 4.09 (m, 2H), 3.66 (t, $J = 4.8$ Hz, 1H), 3.49 (s, 3H), 2.38 (dd, $J = 14.9, 6.8$ Hz, 1H), 2.28 (dd, $J =$

14.9, 6.2 Hz, 1H), 2.01 – 1.75 (m, 5H); ^{13}C NMR (126 MHz, cdcl_3) δ 171.2, 156.5 (q, $J_{\text{C-F}} = 38.1$ Hz), 149.3, 137.3, 135.5, 131.0, 128.8 ($\times 2$), 127.5, 127.4 ($\times 2$), 125.0, 115.4 (q, $J_{\text{C-F}} = 287.9$ Hz), 110.4, 110.2, 66.6, 60.4, 55.3, 52.8, 50.2, 49.9, 44.7, 37.1, 33.0, 32.1, 30.9. IR (NaCl/thin film) 3308, 2951, 2864, 1713, 1475, 1210, 1175 cm^{-1} ; $[\alpha]_{\text{D}}^{25} = +41.4$ ($c = 0.90$, CH_2Cl_2).

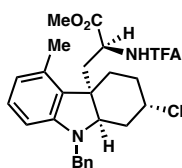
Indoline 247b.



Prepared from 1-benzyl-3-homoallyl-5-methoxy-1*H*-indole and methyl 2-trifluoroacetamidoacrylate using General Procedure A (but with 1.1 equiv ZrCl_4) to yield **246b** in 93% yield. The diastereomeric ratio was determined to be 6:1 by ^1H NMR analysis of the crude reaction mixture. The enantiomeric excess of the major diastereomer was determined to be 91% by chiral SFC analysis (AD-H, 2.5 mL/min, 12% IPA in CO_2 , $\lambda = 254$ nm): t_{R} (major) = 4.5 min; t_{R} (minor) = 4.1 min. The major diastereomer was separated by flash chromatography (15 \rightarrow 20% ethyl acetate/hexanes). ^1H NMR (400 MHz, CDCl_3) δ 7.41 – 7.27 (m, 5H), 6.63 – 6.57 (m, 2H), 6.53 (d, $J = 7.7$ Hz, 1H), 6.39 (d, $J = 8.0$ Hz, 1H), 4.60 (dd, $J = 13.8, 6.8$ Hz, 1H), 4.34 (d, $J = 15.4$ Hz, 1H), 4.23 (dd, $J = 9.8, 6.4$ Hz, 1H), 4.07 (d, $J = 15.4$ Hz, 1H), 3.72 (s, 3H), 3.55 (t, $J = 4.6$ Hz, 1H), 3.47 (s, 3H), 2.44 (dd, $J = 14.9, 7.0$ Hz, 1H), 2.28 (dd, $J = 14.9, 5.8$ Hz, 1H), 2.16 – 2.09 (m, 1H), 1.99 – 1.72 (m, 5H); ^{13}C NMR (101 MHz, CDCl_3) δ 171.3, 156.4 (q, $J_{\text{C-F}} = 37.7$ Hz), 153.4, 144.2, 138.0, 134.7, 128.6 ($\times 2$), 127.5 ($\times 2$), 127.3, 115.4 (q, $J_{\text{C-F}} =$

288.0), 112.7, 109.8, 109.2, 67.0, 55.8, 52.7, 51.2, 50.1, 44.7, 36.9, 33.0, 32.3, 31.1, 29.7; IR (NaCl/thin film) 3315, 2925, 1716, 1555, 1490, 1215, 1176 cm^{-1} ; $[\alpha]_{\text{D}}^{25} = +40.4$ ($c = 0.96$, CH_2Cl_2). HRMS (MM) calc'd for $\text{C}_{26}\text{H}_{28}\text{ClF}_3\text{N}_2\text{O}_4$ $[\text{M}+\text{H}]^+$ 525.1762, found 525.1749.

Indoline 247c.



Prepared from 1-benzyl-3-homoallyl-4-methyl-1*H*-indole and methyl 2-trifluoroacetamidoacrylate using General Procedure A to yield **246c** in 90% yield. The diastereomeric ratio was determined to be 4:1 by ^1H NMR analysis of the crude reaction mixture. The enantiomeric excess of the major diastereomer was determined to be 90% by chiral SFC analysis (OD-H, 2.5 mL/min, 10% EtOH in CO_2 , $\lambda = 254$ nm): t_{R} (major) = 7.5 min; t_{R} (minor) = 6.7 min. The major diastereomer was separated by flash chromatography (5→10% ethyl acetate/hexanes). ^1H NMR (400 MHz, CDCl_3) δ 7.39 – 7.27 (m, 5H), 6.96 (t, $J = 7.7$ Hz, 1H), 6.67 (d, $J = 7.6$ Hz, 1H), 6.48 (d, $J = 7.6$ Hz, 1H), 6.37 (d, $J = 7.9$ Hz, 1H), 4.64 (q, $J = 7.0$ Hz, 1H), 4.40 (d, $J = 15.8$ Hz, 1H), 4.21 – 4.12 (m, 2H), 3.60 (t, $J = 4.3$ Hz, 1H), 3.38 (s, 3H), 2.51 (dd, $J = 15.0, 6.6$ Hz, 1H), 2.40 (dd, $J = 15.0, 7.0$ Hz, 1H), 2.29 (s, 3H), 2.21 (dt, $J = 14.6, 4.3$ Hz, 1H), 2.03 – 1.88 (m, 4H), 1.88 – 1.75 (m, 1H); ^{13}C NMR (101 MHz, CDCl_3) δ 171.3, 156.5 (q, $J_{\text{C-F}} = 37.8$ Hz), 150.9, 138.0, 133.9, 129.7, 128.7 ($\times 2$), 128.3, 127.4 ($\times 2$), 127.3, 122.2, 115.4 (q, $J_{\text{C-F}} = 287.9$ Hz), 107.0, 65.8, 55.5, 52.6, 50.6, 50.4, 46.2, 36.6, 33.1, 31.3, 31.1, 19.1; IR

(NaCl/thin film) 3311, 2953, 1711, 1589, 1452, 1212, 1177 cm^{-1} ; $[\alpha]_{\text{D}}^{25} = 79.4$ ($c = 0.81$, CH_2Cl_2).

Indoline 247d.

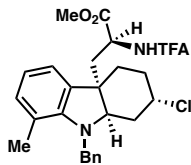


Prepared from 1-benzyl-3-homoallyl-5-methyl-1*H*-indole and methyl 2-trifluoroacetamidoacrylate using General Procedure A to yield **246d** in quantitative yield. The diastereomeric ratio was determined to be 6:1 by ^1H NMR analysis of the crude reaction mixture. The enantiomeric excess of the major diastereomer was determined to be 90% by chiral SFC analysis (OJ-H, 2.5 mL/min, 8% EtOH in CO_2 , $\lambda = 254$ nm): t_{R} (major) = 7.0 min; t_{R} (minor) = 5.1 min. The major diastereomer was separated by flash chromatography. ^1H NMR (500 MHz, CDCl_3) δ 7.39 – 7.27 (m, 5H), 6.87 (ddd, $J = 7.9$, 1.7, 0.7 Hz, 1H), 6.78 (d, $J = 1.7$ Hz, 1H), 6.50 (d, $J = 7.7$ Hz, 1H), 6.39 (d, $J = 7.9$ Hz, 1H), 4.62 (td, $J = 7.6$, 5.5 Hz, 1H), 4.37 (d, $J = 15.4$ Hz, 1H), 4.24 (dt, $J = 11.3$, 3.7 Hz, 1H), 4.10 (d, $J = 15.4$ Hz, 1H), 3.56 (t, $J = 5.2$ Hz, 1H), 3.49 (s, $J = 2.3$ Hz, 3H), 2.44 (dd, $J = 14.8$, 7.5 Hz, 1H), 2.30 – 2.21 (m, 4H), 2.09 – 1.78 (m, 6H); ^{13}C NMR (126 MHz, CDCl_3) δ 171.4, 156.4 (q, $J_{\text{C-F}} = 37.8$ Hz), 147.9, 138.0, 133.0, 128.7, 128.6 ($\times 2$), 128.0, 127.5 ($\times 2$), 127.3, 122.8, 116.6 (q, $J_{\text{C-F}} = 287.8$ Hz), 109.0, 66.9, 56.1, 52.6, 50.4, 50.1, 44.6, 37.3, 32.8, 31.1, 30.8, 20.7; IR (NaCl/thin film) 3314, 2951, 2868, 1715, 1552, 1490, 1440, 1210, 1177 cm^{-1} ; $[\alpha]_{\text{D}}^{25} = +55.3$ ($c = 0.85$, CH_2Cl_2). HRMS (MM) calc'd for $\text{C}_{26}\text{H}_{28}\text{ClF}_3\text{N}_2\text{O}_3$ $[\text{M}+\text{H}]^+$ 509.1813, found 509.1831.

Indoline 247e.

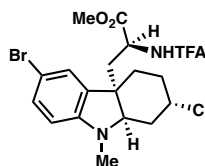
Prepared from 1-benzyl-3-homoallyl-6-methyl-1*H*-indole and methyl 2-trifluoroacetamidoacrylate using General Procedure A (but with 1.1 equiv ZrCl_4) to yield **246e** in 74% yield. The diastereomeric ratio was determined to be 3:1 by ^1H NMR analysis of the crude reaction mixture. The enantiomeric excess of the major diastereomer was determined to be 92% by chiral SFC analysis (AD-H, 2.5 mL/min, 20% IPA in CO_2 , $\lambda = 254$ nm): $t_{\text{R}}(\text{major}) = 2.6$ min; $t_{\text{R}}(\text{minor}) = 2.1$ min. The major diastereomer was separated by flash chromatography (5 \rightarrow 10% ethyl acetate/hexanes). ^1H NMR (500 MHz, CDCl_3) δ 7.39 – 7.27 (m, 5H), 6.84 (d, $J = 7.4$ Hz, 1H), 6.54 (d, $J = 7.4$ Hz, 1H), 6.49 (d, $J = 7.7$ Hz, 1H), 6.33 (s, 1H), 4.60 (td, $J = 7.7, 5.4$ Hz, 1H), 4.38 (d, $J = 15.6$ Hz, 1H), 4.21 (dq, $J = 11.0, 3.7$ Hz, 1H), 4.13 (d, $J = 15.6$ Hz, 1H), 3.58 (t, $J = 5.3$ Hz, 1H), 3.49 (s, $J = 2.4$ Hz, 3H), 2.39 (dd, $J = 14.8, 7.6$ Hz, 1H), 2.27 – 2.21 (m, 4H), 2.06 – 1.77 (m, 6H); ^{13}C NMR (126 MHz, CDCl_3) δ 171.4, 156.5 (q, $J_{\text{C-F}} = 37.8$ Hz), 150.3, 138.6, 138.0, 129.9, 128.7 ($\times 2$), 127.4 ($\times 2$), 127.3, 121.8, 119.2, 115.4 (q, $J_{\text{C-F}} = 287.8$ Hz), 109.8, 66.7, 56.0, 52.7, 50.1, 50.0, 44.37, 37.6, 33.0, 31.0, 30.8, 21.7; IR (NaCl/thin film) 3312, 2950, 1712, 1612, 1551, 1493, 1452, 1210, 1176 cm^{-1} ; $[\alpha]_{\text{D}}^{25} = +65.8$ ($c = 0.89$, CH_2Cl_2). HRMS (MM) calc'd for $\text{C}_{26}\text{H}_{28}\text{ClF}_3\text{N}_2\text{O}_3$ $[\text{M}+\text{H}]^+$ 509.1813, found 509.1823.

Indoline 247f.



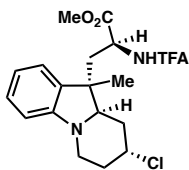
Prepared from 1-benzyl-3-homoallyl-7-methyl-1*H*-indole and methyl 2-trifluoroacetamidoacrylate using General Procedure A to yield **246f** in 89% yield. The diastereomeric ratio was determined to be 6:1 by ¹H NMR analysis of the crude reaction mixture. The enantiomeric excess of the major diastereomer was determined to be 89% by chiral SFC analysis (AD-H, 2.5 mL/min, 20% IPA in CO₂, λ = 254 nm): *t*_R(major) = 2.7 min; *t*_R(minor) = 2.2 min. The major diastereomer was separated by flash chromatography (5→10% ethyl acetate/hexanes). ¹H NMR (400 MHz, CDCl₃) δ 7.39 – 7.27 (m, 5H), 6.91 (d, *J* = 7.5 Hz, 1H), 6.82 (d, *J* = 7.3 Hz, 1H), 6.70 (t, *J* = 7.4 Hz, 1H), 6.46 (d, *J* = 7.8 Hz, 1H), 4.71 (d, *J* = 16.5 Hz, 1H), 4.62 – 4.49 (m, 2H), 4.19 (td, *J* = 7.9, 3.8 Hz, 1H), 3.51 (s, 3H), 3.45 (t, *J* = 4.9 Hz, 1H), 2.35 (s, 3H), 2.24 (d, *J* = 6.3 Hz, 2H), 2.04 (dt, *J* = 15.0, 4.4 Hz, 1H), 1.96 – 1.69 (m, 5H).; ¹³C NMR (101 MHz, CDCl₃) δ 171.4, 156.4 (q, *J*_{C-F} = 37.7 Hz), 148.0, 139.3, 133.7, 132.3, 128.7 (×2), 127.3, 127.2 (×2), 120.4, 120.0, 119.3, 115.4 (q, *J*_{C-F} = 287.8 Hz), 66.4, 55.9, 52.7, 52.3, 50.0, 44.6, 37.9, 33.9, 32.0, 30.8, 19.6; IR (NaCl/thin film) 3314, 2952, 1715, 1558, 1452, 1208, 1176 cm⁻¹; [α]_D²⁵ = +57.2 (*c* = 0.94, CH₂Cl₂). HRMS (MM) calc'd for C₂₆H₂₈ClF₃N₂O₃ [M-H]⁻ 507.1668, found 507.1681.

5-Bromo-N-methyl Indoline.



Prepared from 1-methyl-3-homoallyl-5-bromo-1*H*-indole and methyl 2-trifluoroacetamidoacrylate using General Procedure A to yield **247** in 77% yield. The diastereomeric ratio was determined to be 5:1 by ¹H NMR analysis of the crude reaction mixture. The enantiomeric excess of the major diastereomer was determined to be 88% by chiral SFC analysis (AD-H, 2.5 mL/min, 20% MeOH in CO₂, λ = 254 nm): *t*_R(major) = 1.9 min; *t*_R(minor) = 5.3 min. The major diastereomer was separated by flash chromatography. ¹H NMR (500 MHz, CDCl₃) δ 7.23 (dd, *J* = 8.3, 2.0 Hz, 1H), 7.02 (d, *J* = 2.0 Hz, 1H), 6.81 (d, *J* = 7.9 Hz, 1H), 6.41 (d, *J* = 8.3 Hz, 1H), 4.56 (dd, *J* = 14.4, 6.7 Hz, 1H), 4.25 – 4.17 (m, 1H), 3.54 (s, *J* = 2.4 Hz, 3H), 3.47 (t, *J* = 4.9 Hz, 1H), 2.70 (s, 3H), 2.36 (dd, *J* = 15.0, 7.0 Hz, 1H), 2.23 (ddd, *J* = 15.0, 5.9, 2.7 Hz, 1H), 2.15 – 2.07 (m, 1H), 2.03 – 1.96 (m, 1H), 1.93 – 1.74 (m, 4H); ¹³C NMR (126 MHz, CDCl₃) δ 171.1, 156.5 (q, *J*_{C-F} = 37.9 Hz), 150.1, 135.6, 131.1, 124.9, 115.5 (q, *J*_{C-F} = 287.5 Hz), 110.4, 110.1, 68.7, 55.2, 52.7, 50.1, 44.7, 37.7, 32.9, 32.8, 32.4, 31.0.; IR (NaCl/thin film) 3309, 2953, 2863, 1709, 1555, 1478, 1210, 1178 cm⁻¹; [α]_D²⁵ = +23.7 (*c* = 0.88, CH₂Cl₂). HRMS (MM) calc'd for C₁₉H₂₁BrClF₃N₂O₃ [M+H]⁺ 497.0449, found 497.0452.

Indoline 248.

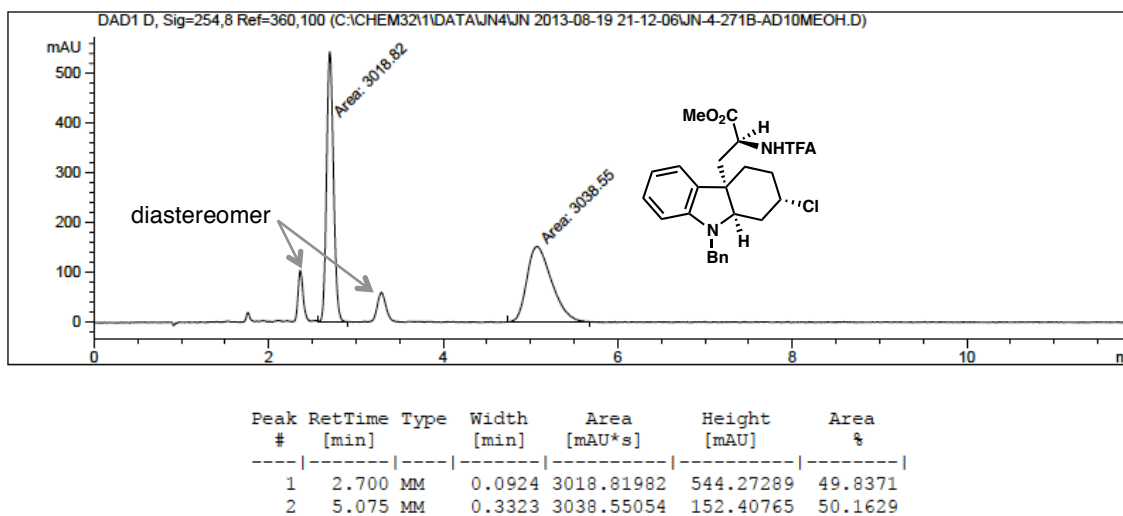


Prepared from 1-homoallyl-3-methyl-1*H*-indole and methyl 2-trifluoroacetamidoacrylate using General Procedure A to yield **248** in 80% yield. The diastereomeric ratio was determined to be 6:1 by ¹H NMR analysis of the crude reaction mixture. The

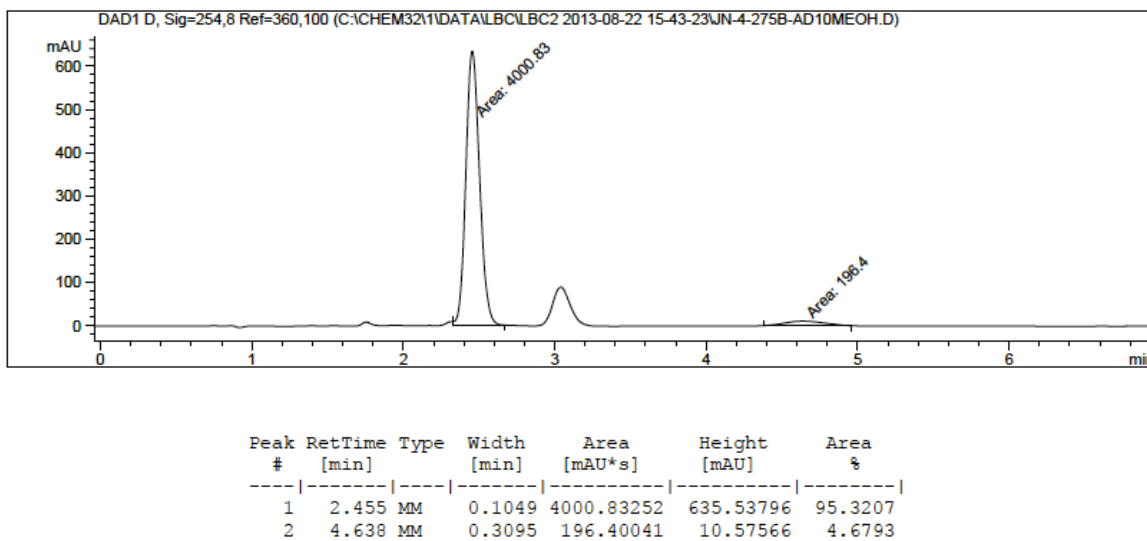
enantiomeric excess of the major diastereomer was determined to be 89% by chiral SFC analysis (AD-H, 2.5 mL/min, 10% IPA in CO₂, λ = 254 nm): t_R (major) = 2.7 min; t_R (minor) = 8.7 min. The major diastereomer was separated by flash chromatography (12→15% ethyl acetate/hexanes). ¹H NMR (500 MHz, CDCl₃) δ 7.12 (td, J = 7.7, 1.2 Hz, 1H), 6.99 (dd, J = 7.7, 1.3 Hz, 1H), 6.89 (d, J = 7.9 Hz, 1H), 6.74 (td, J = 7.4, 0.9 Hz, 1H), 6.50 (d, J = 7.9 Hz, 1H), 4.58 (td, J = 7.8, 4.6 Hz, 1H), 3.98 (tt, J = 11.8, 4.0 Hz, 1H), 3.72 (ddd, J = 13.3, 4.7, 2.1 Hz, 1H), 3.59 (s, J = 3.5 Hz, 3H), 3.16 (dd, J = 11.8, 2.7 Hz, 1H), 2.82 (tt, J = 18.4, 9.2 Hz, 1H), 2.30 (dd, J = 14.9, 4.7 Hz, 1H), 2.21 – 2.07 (m, 3H), 1.89 – 1.77 (m, 1H), 1.72 (q, J = 11.9 Hz, 1H), 1.22 (s, 3H); ¹³C NMR (126 MHz, CDCl₃) δ 171.3, 156.6 (q, J_{C-F} = 37.7 Hz), 148.8, 134.4, 128.5, 122.7, 118.8, 115.5 (q, J_{C-F} = 287.7 Hz), 107.3, 70.1, 57.1, 52.7, 50.3, 45.7, 43.9, 40.4, 35.9, 34.6, 21.0; IR (NaCl/thin film) 3314, 2958, 1711, 1606, 1482, 1454, 1211, 1173 cm⁻¹. HRMS (MM) calc'd for C₁₉H₂₂ClF₃N₂O₃ [M+H]⁺ 419.1344, found 419.1342.

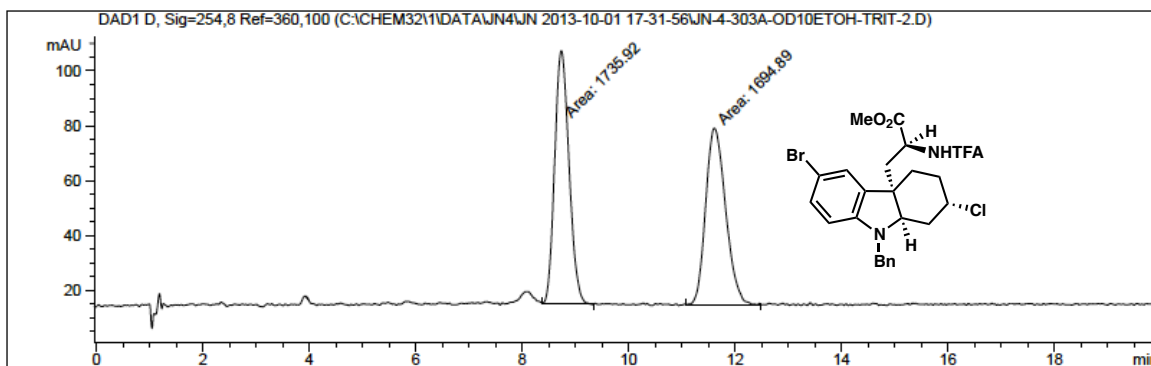
4.4.4 SFC Traces for Racemic and Enantioenriched Products

246 (Table 7, Entry 8): racemic

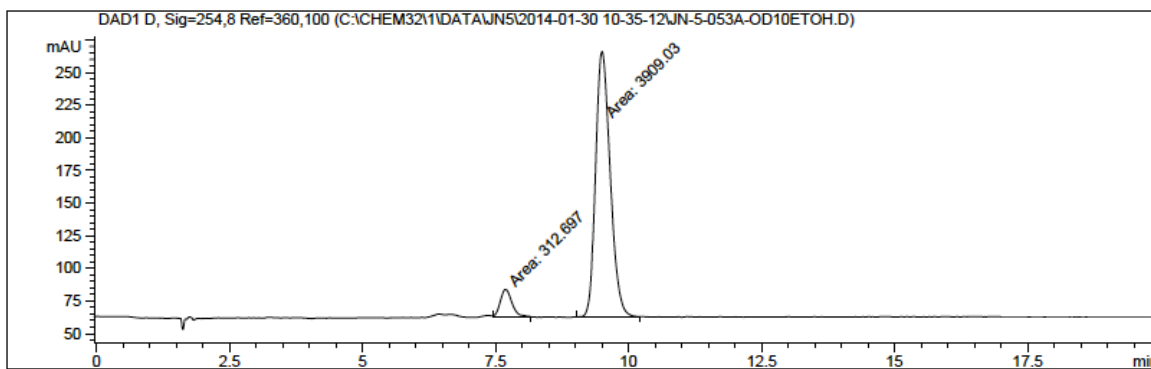


246 (Table 7, Entry 8): 91% ee

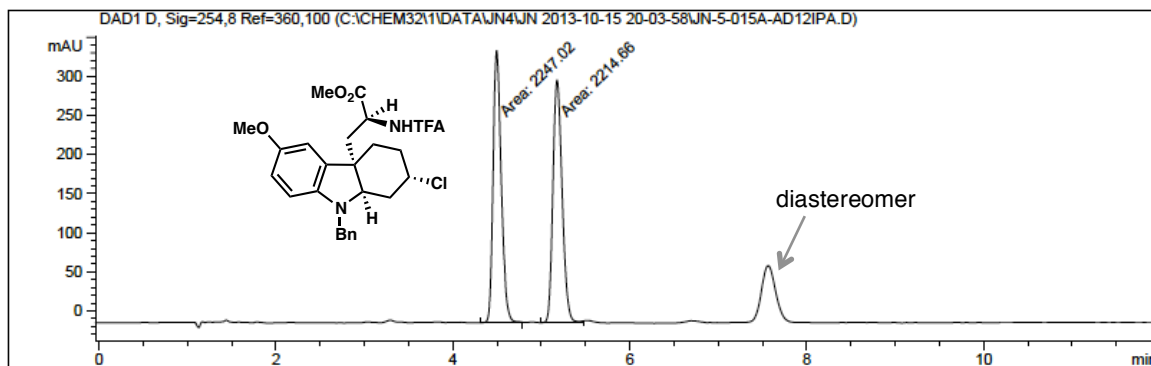


247a (Table 8): racemic

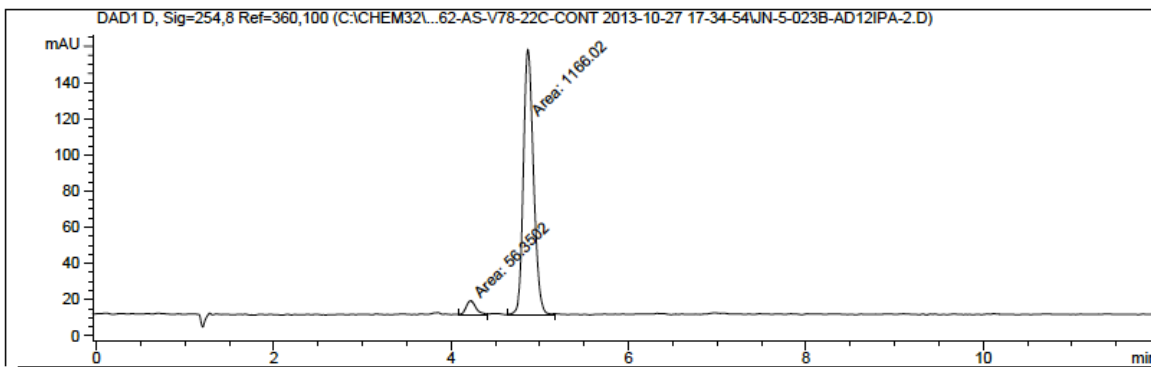
Peak #	RetTime [min]	Type	Width [min]	Area [mAU*s]	Height [mAU]	Area %
1	8.739	MM	0.3135	1735.92102	92.27703	50.5979
2	11.611	MM	0.4383	1694.89441	64.44508	49.4021

247a (Table 8, major diastereomer only): 85% ee

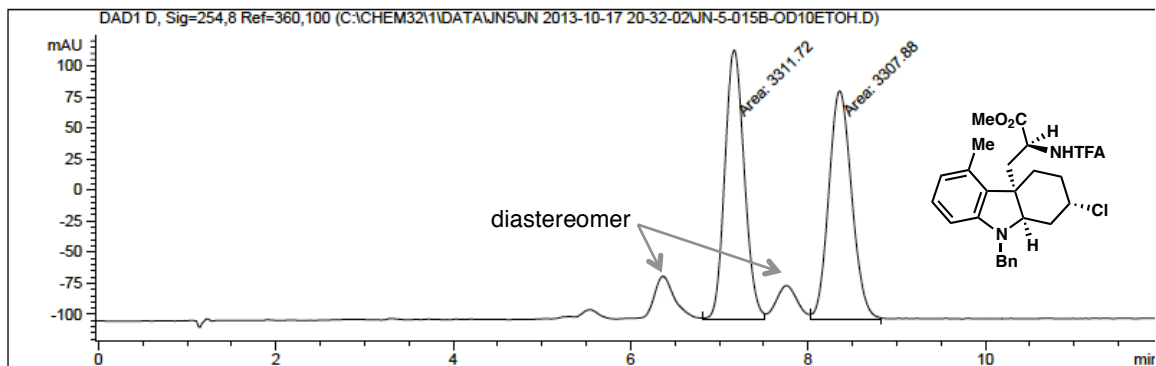
Peak #	RetTime [min]	Type	Width [min]	Area [mAU*s]	Height [mAU]	Area %
1	7.690	MM	0.2497	312.69736	20.87528	7.4069
2	9.505	MM	0.3200	3909.02954	203.61522	92.5931

247b (Table 8): racemic

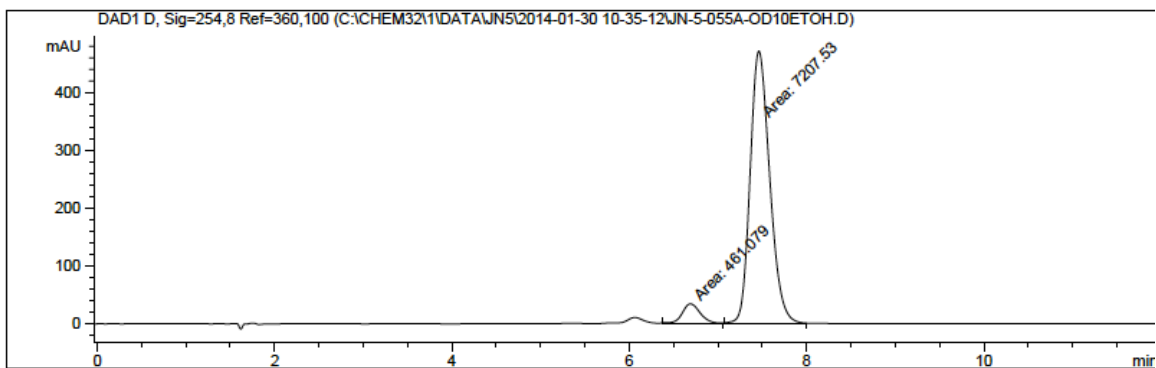
Peak #	RetTime [min]	Type	Width [min]	Area [mAU*s]	Height [mAU]	Area %
1	4.496	MM	0.1072	2247.02026	349.30011	50.3626
2	5.178	MM	0.1193	2214.66113	309.27405	49.6374

247b (Table 8): 91% ee

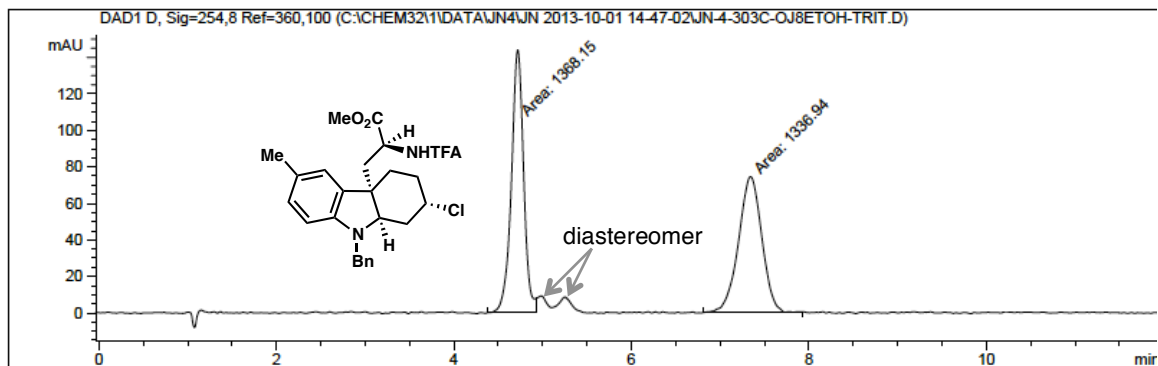
Peak #	RetTime [min]	Type	Width [min]	Area [mAU*s]	Height [mAU]	Area %
1	4.219	MM	0.1233	56.35015	7.61557	4.6099
2	4.866	MM	0.1325	1166.02209	146.64792	95.3901

247c (Table 8): racemic

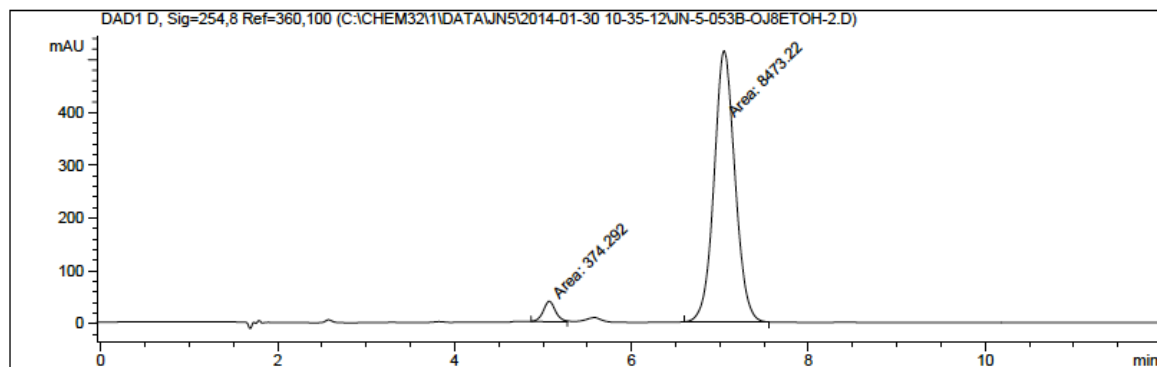
Peak #	RetTime [min]	Type	Width [min]	Area [mAU*s]	Height [mAU]	Area %
1	7.167	MM	0.2547	3311.72388	216.69806	50.0291
2	8.356	MM	0.3001	3307.87622	183.70784	49.9709

247c (Table 8, major diastereomer only): 88% ee

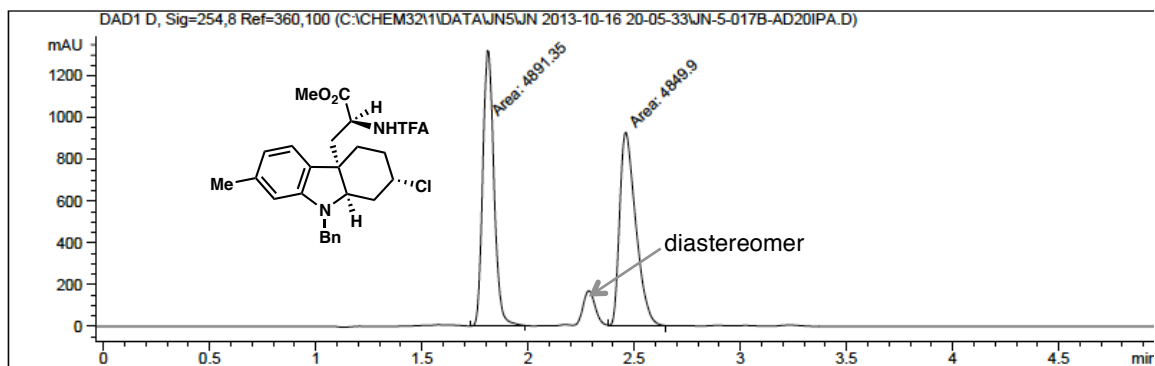
Peak #	RetTime [min]	Type	Width [min]	Area [mAU*s]	Height [mAU]	Area %
1	6.689	MM	0.2305	461.07950	33.33388	6.0126
2	7.461	MM	0.2553	7207.52832	470.58481	93.9874

247d (Table 8): racemic

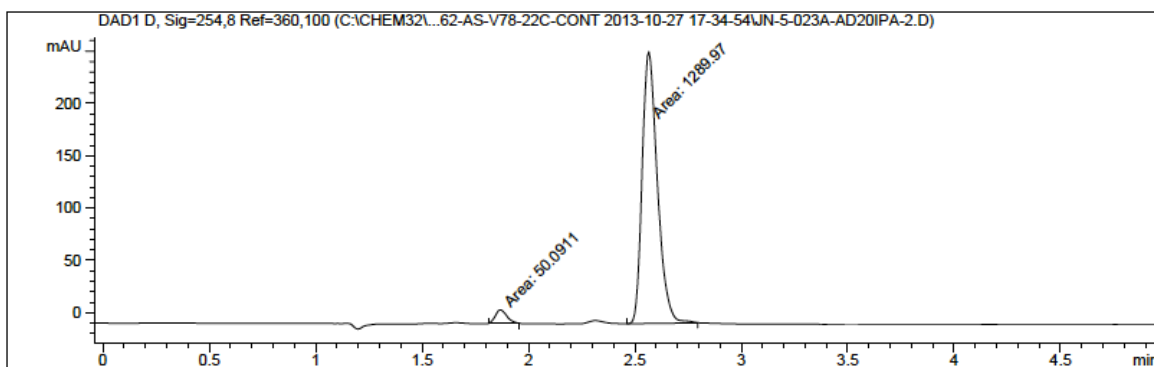
Peak #	RetTime [min]	Type	Width [min]	Area [mAU*s]	Height [mAU]	Area %
1	4.720	MM	0.1588	1368.15161	143.62547	50.5769
2	7.343	MM	0.3010	1336.93970	74.03839	49.4231

247d (Table 8): 92% ee

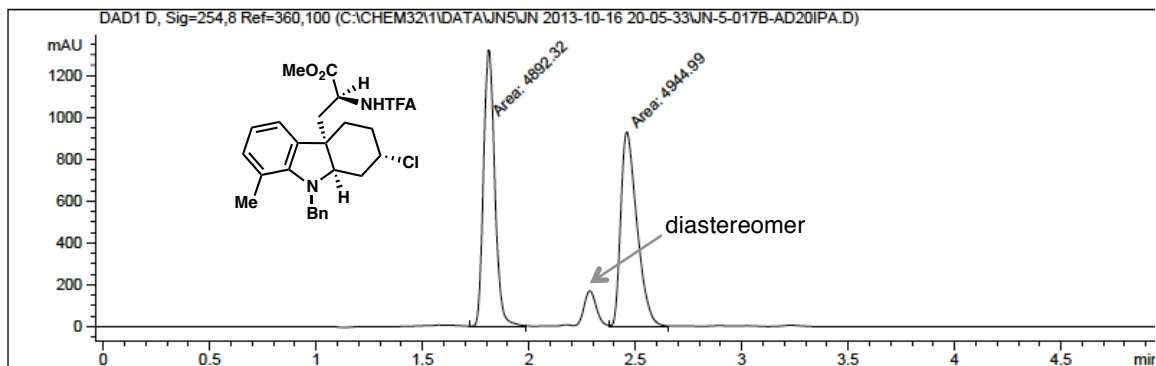
Peak #	RetTime [min]	Type	Width [min]	Area [mAU*s]	Height [mAU]	Area %
1	5.071	MM	0.1609	374.29236	38.77222	4.2305
2	7.047	MM	0.2750	8473.22168	513.56281	95.7695

247e (Table 8): racemic

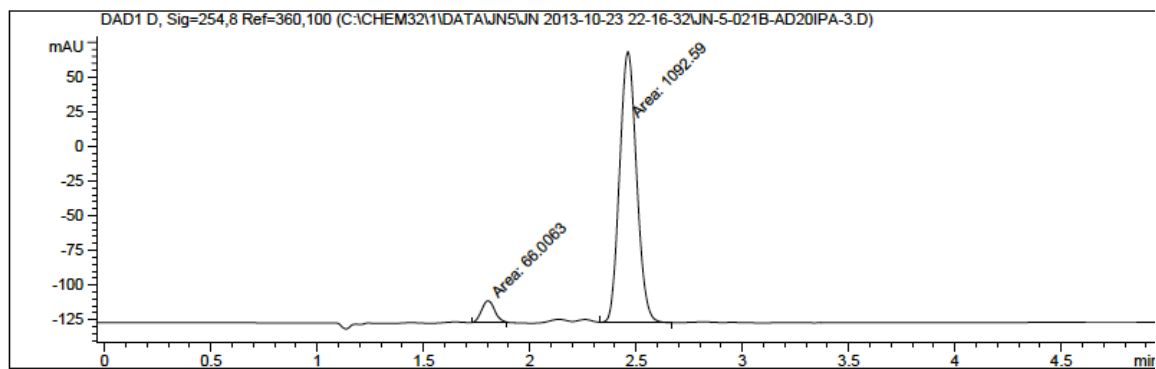
Peak #	RetTime [min]	Type	Width [min]	Area [mAU*s]	Height [mAU]	Area %
1	1.812	MM	0.0605	4891.34961	1347.66492	50.2127
2	2.461	MM	0.0868	4849.90088	931.37439	49.7873

247e (Table 8): 93% ee

Peak #	RetTime [min]	Type	Width [min]	Area [mAU*s]	Height [mAU]	Area %
1	1.869	MM	0.0635	50.09111	13.15408	3.7380
2	2.565	MM	0.0826	1289.97192	260.39725	96.2620

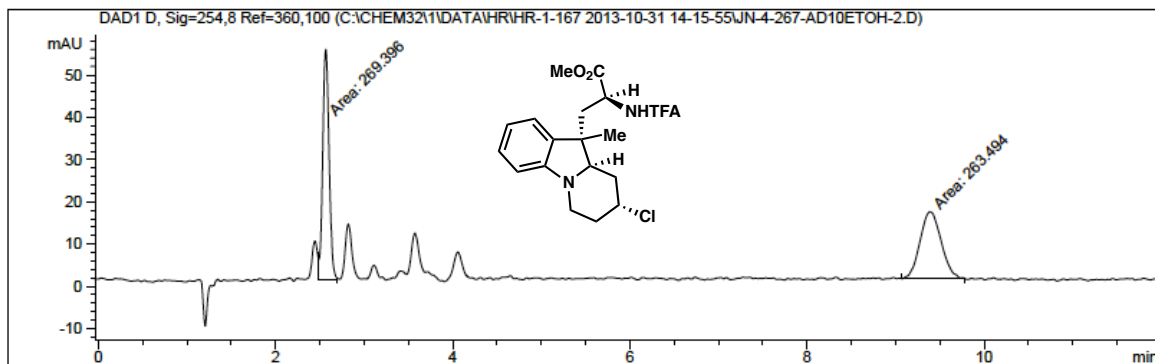
247f (Table 8): racemic

Peak #	RetTime [min]	Type	Width [min]	Area [mAU*s]	Height [mAU]	Area %
1	1.812	MM	0.0610	4892.31689	1336.32910	49.7323
2	2.460	MM	0.0883	4944.98926	933.73901	50.2677

247f (Table 8): 89% ee

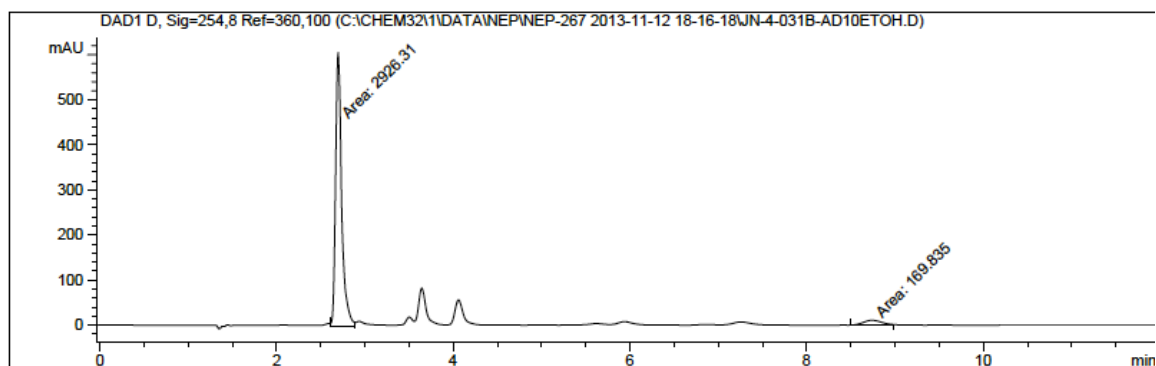
Peak #	RetTime [min]	Type	Width [min]	Area [mAU*s]	Height [mAU]	Area %
1	1.804	MM	0.0707	66.00635	15.56793	5.6971
2	2.462	MM	0.0929	1092.58643	196.06543	94.3029

248 (Table 8): racemic

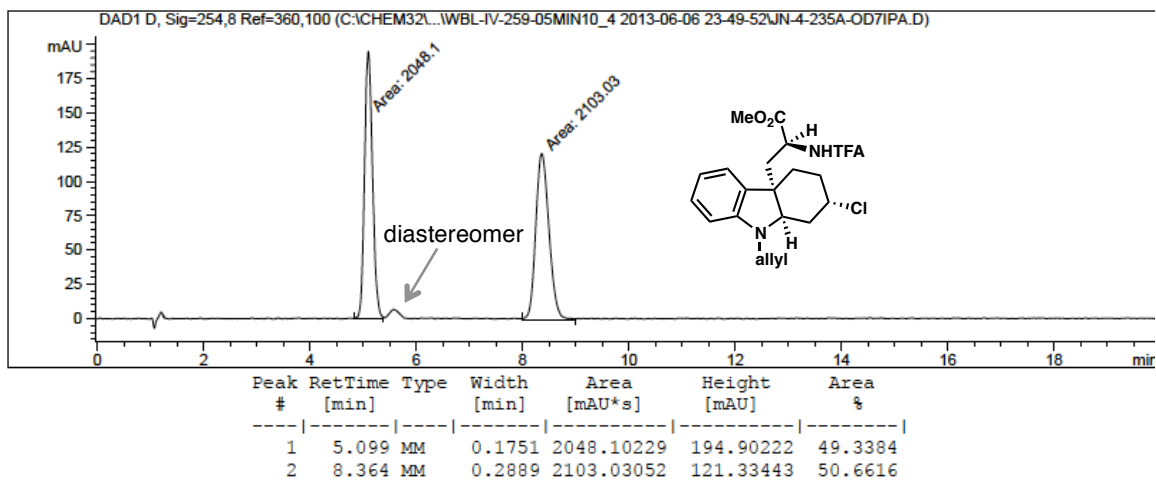
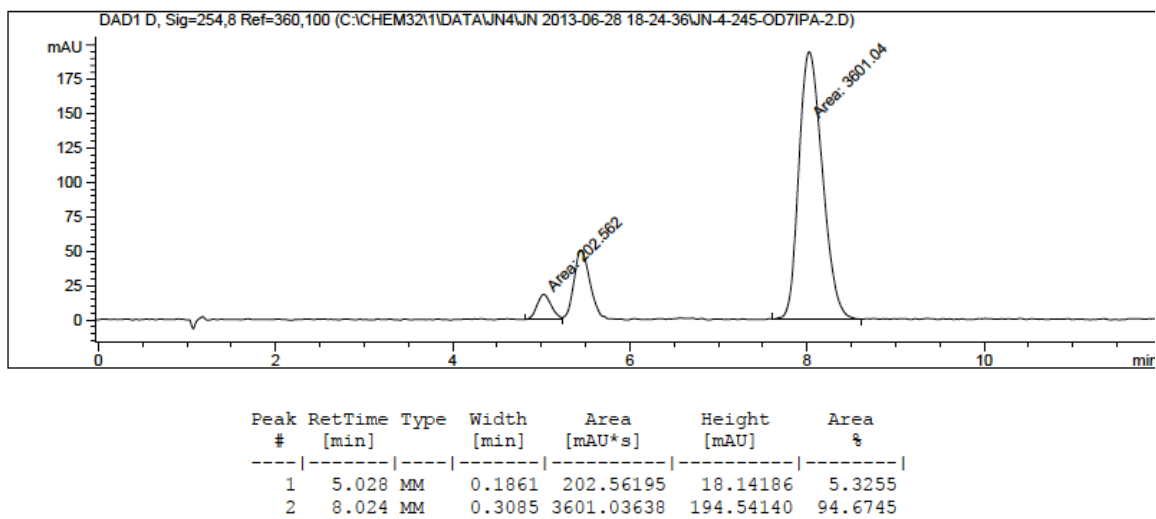


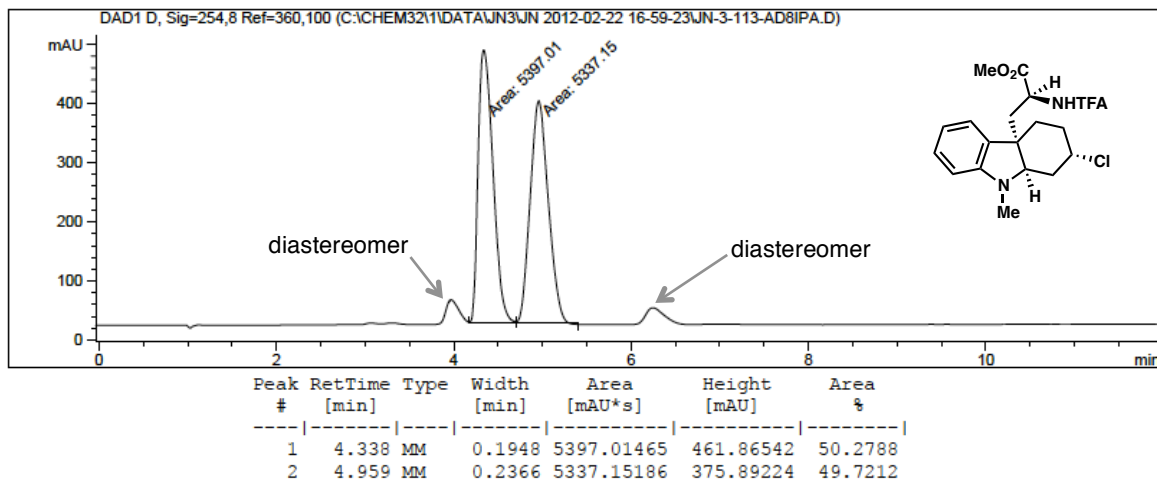
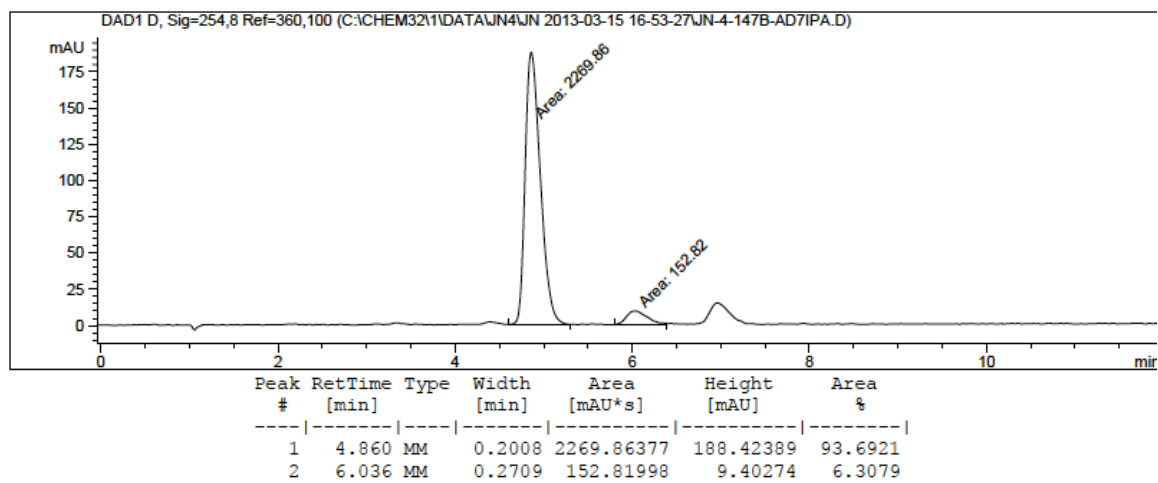
Peak #	RetTime [min]	Type	Width [min]	Area [mAU*s]	Height [mAU]	Area %
1	2.566	MM	0.0822	269.39600	54.61353	50.5538
2	9.388	MM	0.2768	263.49390	15.86486	49.4462

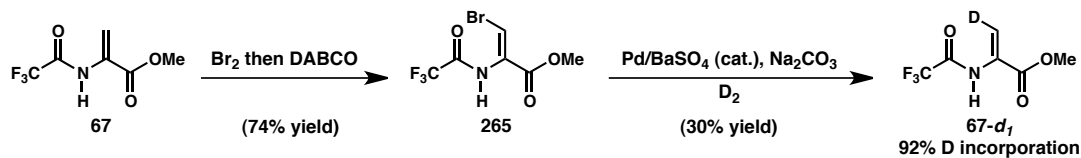
248 (Table 8): 89% ee



Peak #	RetTime [min]	Type	Width [min]	Area [mAU*s]	Height [mAU]	Area %
1	2.698	MM	0.0800	2926.30688	609.68549	94.5146
2	8.746	MM	0.2511	169.83505	11.27103	5.4854

245 (Table 8): racemic**245** (Table 8): 89% ee

169 (Table 8): racemic**169** (Table 8): 87% ee

4.4.5 Synthesis of deuterated acrylate **67-d₁**

Acrylate **67** (10 mmol, 1.97g, 1.0 equiv) was dissolved in 50 mL CH₂Cl₂ and cooled to -78 °C. Molecular bromine (10 mmol, 0.51 mL, 1.0 equiv) was added dropwise, and the reaction was stirred for 10 minutes before moving to an ice bath, where it was stirred for 40 minutes. DABCO (10 mmol, 1.1 g, 1.0 equiv) was added as a solution in 15 mL CH₂Cl₂. The reaction was stirred for 1.5 h, then filtered through celite, and concentrated. The crude mixture was purified by flash chromatography (30% Et₂O/pentane) to yield 2.03 g (74% yield) of bromoacrylate **285**.

285: ¹H NMR (300 MHz, acetone) δ 7.89 (s, 1H), 3.80 (s, 3H)

Bromoacrylate **285** (3 mmol, 830 mg) was dissolved in 6 mL ethyl acetate (not dried), and Pd/BaSO₄ (reduced, 29 mg) was added. The reaction was sparged with D₂, then sealed and stirred until the reaction no longer progressed by TLC (approximately four days). The reaction was filtered through celite, concentrated, and purified by flash chromatography (20% Et₂O/pentane) to yield 180.5 mg (30% yield) of deuterium labelled acrylate **67-d₁**.

67-d₁: ¹H NMR (500 MHz, CDCl₃) δ 8.53 (s, 1H), 6.13 (d, *J* = 1.4 Hz, 1H), 3.92 (s, 3H);

¹³C NMR (126 MHz, CDCl₃) δ 163.5, 155.1 (q, *J*_{C-F} = 38.2 Hz), 129.4, 115.2 (q, *J*_{C-F} = 288.3 Hz), 112.1 (t, *J*_{C-D} = 26 Hz), 53.47; HRMS (MM) calc'd for C₆H₅DF₃N₂O₃ [M-H]⁻ 197.0290, found 197.0295.

4.5 Notes and References

- (1) (a) Heathcock, C. H. *Proceedings of the National Academy of Sciences* **1996**, *93*, 14323–14327. (b) Heathcock, C. H.; Hansen, M. M.; Ruggeri, R. B.; Kath, J. C. *J. Org. Chem.* **1992**, *57*, 2544–2553. (c) Heathcock, C. H.; Piettre, S.; Ruggeri, R. B.; Ragan, J. A.; Kath, J. C. *J. Org. Chem.* **1992**, *57*, 2554–2566. (d) Heathcock, C. H. *Angew. Chem. Int. Ed. Engl.* **1992**, *31*, 665–681.
- (2) He, F.; Bo, Y.; Altom, J. D.; Corey, E. J. *J. Am. Chem. Soc.* **1999**, *121*, 6771–6772.
- (3) (a) MacMillan, D. W.; Overman, L. E.; Pennington, L. D. *J. Am. Chem. Soc.* **2001**, *123*, 9033–9044; (b) Overman, L. E.; Pennington, L. D. *Org. Lett.* **2000**, *2*, 2683–2686; (c) Gallou, F.; MacMillan, D. W.; Overman, L. E.; Paquette, L. A.; Pennington, L. D.; Yang, J. *Org. Lett.* **2001**, *3*, 135–137.
- (4) Kopecky, D. J.; Rychnovsky, S. D. *J. Am. Chem. Soc.* **2001**, *123*, 8420–8421.
- (5) Van Orden, L. J.; Patterson, B. D.; Rychnovsky, S. D. *J. Org. Chem.* **2007**, *72*, 5784–5793.
- (6) Reddy, B. V. S.; Borkar, P.; Yadav, J. S.; Sridhar, B.; Grée, R. *J. Org. Chem.* **2011**, *76*, 7677–7690.
- (7) (a) Ishitani, H.; Komiyama, S.; Kobayashi, S. *Angew. Chem. Int. Ed. Engl.* **1998**, *37*, 3186–3188; (b) Ishitani, H.; Komiyama, S.; Hasegawa, Y.; Kobayashi, S. *J. Am. Chem. Soc.* **2000**, *122*, 762–766; (c) Kobayashi, S.; Ishitani, H. *Chirality* **2000**, *12*, 540–543.
- (8) (a) Ishitani, H.; Ueno, M.; Kobayashi, S. *J. Am. Chem. Soc.* **1997**, *119*, 7153–7154; (b) Ishitani, H.; Kitazawa, T.; Kobayashi, S. *Tetrahedron Letters* **1999**, *40*, 2161–2164; (c) Kobayashi, S.; Ishitani, H.; Yamashita, Y.; Ueno, M.; Shimizu, H. *Tetrahedron* **2001**, *57*, 861–866; (d) Ihori, Y.; Yamashita, Y.; Ishitani, H.; Kobayashi, S. *J. Am. Chem. Soc.* **2005**, *127*, 15528–15535; (e) Saruhashi, K.; Kobayashi, S. *J. Am. Chem. Soc.* **2006**, *128*, 11232–11235; (f) Xue, S.; Yu, S.; Deng, Y.; Wulff, W. D. *Angew. Chem. Int. Ed. Engl.* **2001**, *40*, 2271–2274. (g) Mouhtady, O.; Gaspard-Iloughmane, H.; Laporterie, A.; Roux, C. L. *Tetrahedron Letters* **2006**, *47*, 4125–4128.
- (9) (a) Yamashita, Y.; Ishitani, H.; Shimizu, H.; Kobayashi, S. *J. Am. Chem. Soc.* **2002**, *124*, 3292–3302; (b) Kobayashi, J.; Nakamura, M.; Mori, Y.; Yamashita, Y.; Kobayashi, S. *J. Am. Chem. Soc.* **2004**, *126*, 9192–9193; (c) Yao, W.; Wang, J. *Org. Lett.* **2003**, *5*, 1527–1530; (d) Schneider, C.; Hansch, M. *Synlett* **2003**, *2003*, 0837–0840; (e) Schneider, C.; Hansch, M.; Sreekumar, P. *Tetrahedron: Asymmetry* **2006**, *17*, 2738–2742.
- (10) Casolari, S.; Cozzi, P. G.; Orioli, P. *Chem. Commun.* **1997**, 2123–2124.

- (11) (a) Kobayashi, S.; Kusakabe, K.-I.; Komiyama, S.; Ishitani, H. *J. Org. Chem.* **1999**, *64*, 4220–4221; (b) Kobayashi, S.; Shimizu, H.; Yamashita, Y.; Ishitani, H.; Kobayashi, J. *J. Am. Chem. Soc.* **2002**, *124*, 13678–13679; (c) Yamashita, Y.; Saito, S.; Ishitani, H.; Kobayashi, S. *J. Am. Chem. Soc.* **2003**, *125*, 3793–3798.
- (12) Ishihara, K.; Nakamura, S.; Kaneeda, M.; Yamamoto, H. *J. Am. Chem. Soc.* **1996**, *118*, 12854–12855.
- (13) Fehr, C.; Stempf, I.; Galindo, J. *Angew. Chem. Int. Ed. Engl.* **1993**, *32*, 1044–1046.
- (14) Vedejs, E.; Kruger, A. W. *J. Org. Chem.* **1998**, *63*, 2792–2793.
- (15) Hanessian, S.; Tremblay, M.; Petersen, J. F. W. *J. Am. Chem. Soc.* **2004**, *126*, 6064–6071.